

**A STUDY OF SOLID CO₂ FORMATION FROM RAPID FLUID
EXPANSION USING CFD AND MATHEMATICAL
MODELLING**

EDDIE CHANG JEE TED

12562

**CHEMICAL ENGINEERING
UNIVERSITI TEKNOLOGI PETRONAS**

AUGUST 2013

CERTIFICATION OF APPROVAL

A Study of Solid CO₂ Formation from Rapid Fluid Expansion using CFD and Mathematical Modeling

by

Eddie Chang Jee Ted

A project dissertation submitted to the
Chemical Engineering Programme
Universiti Teknologi PETRONAS
in partial fulfillment of the requirement for the
BACHELOR OF ENGINEERING (Hons)
(CHEMICAL ENGINEERING)

Approved by,



(DR. RISZA BTE RUSLI)

UNIVERSITI TEKNOLOGI PETRONAS

TRONOH, PERAK

August 2013

CERTIFICATION OF ORIGINALITY

This is to certify that I am responsible for the work submitted in this project, that the original work is my own except as specified in the references and acknowledgements, and that the original work contained herein have not been undertaken or done by unspecified sources or persons.



EDDIE CHANG JEE TED

ACKNOWLEDGEMENT

The completion of this final year project will not be possible without the support of many individuals and organizations. First and foremost, I would like to extend my most sincere gratitude to my supervisor, Dr. Risza binti Rusli, who never stops believing in me. Her advice, guidance, and constant words of encouragement are what pushes me to achieve all of my goals for this project. My appreciation goes to Mr. Ban Zhen Hong and Ms. Tan Lian See, who have tirelessly provided me with useful information and suggestions to solve my problems. Many thanks to Dr. Azmi bin Mohd Shariff and Ms. Noorfidza Yub Harun, whose constructive criticisms have helped make this project much more valuable. My warmest gratitude is extended to my good friends, Lee Yi Tong, Rachelle Then and Low Huei Ming, who have supported me since the instigation of this project, and cheered me on to overcome every obstacle that has come my way. Lastly, I could never say enough thanks to my family, whose love is unyielding and knows no boundary.

TABLE OF CONTENTS

ABSTRACT	1
CHAPTER 1: INTRODUCTION	2
1.1 Background of Study	2
1.2 Problem Statement	4
1.3 Objectives and Scope of Study	4
1.4 Relevancy and Feasibility of Project	5
CHAPTER 2: LITERATURE REVIEW	6
CHAPTER 3: THEORY	9
CHAPTER 4: RESEARCH METHODOLOGY	13
4.1 Project Activities	13
4.2 Boundary Conditions	14
4.3 CFD Simulation using FLUENT 14.0	16
4.4 Mathematical Modeling	20
4.5 Key Milestones	21
4.6 Gantt Chart	22
CHAPTER 5: RESULTS AND DISCUSSION	23
5.1 CFD Simulation	23
5.2 Mathematical Calculation	27
5.3 Model Validation	31
5.4 Parametric Study for Validation of Trends	32
5.5 Supercritical Release	34
CHAPTER 6: CONCLUSION	36

CHAPTER 7:	REFERENCES	40
CHAPTER 8:	APPENDICES	42
	I	CO ₂ Vapor Pressure Diagram	43
	II	0.5 mm Diameter Nozzle	44
	III	0.1 – 0.4 mm Diameter Nozzle	48
	IV	0.1 – 2 mm Diameter Nozzle (Supercritical)	64

LIST OF FIGURES

Figure 1: Rapid gas expansion of carbon dioxide	3
Figure 2: Process of solid particles formation from liquid droplets	12
Figure 3: Schematic diagram of Liu et al. (2012) experimental apparatus	14
Figure 4: Cross-section of an expansion nozzle	14
Figure 5: Physical geometry of the CFD simulation	16
Figure 6: Emulation of experimental layout by Liu et al. (2012) experimental setup	16
Figure 7: Tetrahedral meshing of geometry	17
Figure 8: Close-up view of the CO ₂ inlet (point of release)	17
Figure 9: Modification of FLUENT material database	18
Figure 10: Flow chart of mathematical model	20
Figure 11: Scaled residuals plot for 360 iterations	23
Figure 12: Temperature contours of CO ₂ discharge at the point of release	24
Figure 13: X-Y plot of jet temperature vs. distance from point of release	24
Figure 14: X-Y plot of jet velocity vs. distance from the point of release	25
Figure 15: Temperature profile for 0.5 mm nozzle CO ₂ release	25
Figure 16: Velocity profile for 0.5 mm nozzle CO ₂ release	26
Figure 17: Validation of model against Liu et al. (2010) for 0.2 mm diameter nozzle	31
Figure 18: Effect of nozzle diameter on droplet size distribution	32
Figure 19: Effect of nozzle diameter on particle size formation	33
Figure 20: Particle size formation at supercritical storage condition (310 K and 150 bar)	34
Figure 21: Experimental apparatus and setup	37
Figure 22: Dry ice particles in jet flow	38
Figure 23: Dry ice particles trapped on glass surface	38
Figure 24: Carbon dioxide vapor pressure graph	43

LIST OF TABLES

Table 1: Physical properties of carbon dioxide	27
Table 2: Validation of model against Liu et al. (2012)	31

ABSTRACT

Rapid carbon dioxide expansion from an accidental pipeline leakage is an adiabatic process that forms solid CO₂ micro-particles entrained in CO₂ vapor. While the vapor is subsequently dispersed as vapor cloud, the micro-particles – at sizes larger than 100 μm – can rain out to form a solid pool. The pool will then sublime to the atmosphere and contribute significantly to the concentration of vapor cloud. Ultimately, the effect of solid rainout pool on vapor cloud concentration and dispersion has to be taken into consideration when calculating safety distance. In order to investigate the sizes of solid micro-particles formed under varying discharge scenarios, the process of rapid fluid expansion through an orifice (leakage) is emulated using a simulation model. It involves an integration of two sub-models: (1) a 3-D Computational Fluid Dynamics (CFD) model using FLUENT 14.0, and (2) a mathematical model published by authors Hulsbosch-Dam, Spruijt, Necci & Cozzani (2012). The CFD model employs the FLUENT software to obtain temperature and velocity profiles of rapid fluid expansion. The mathematical model calculates the droplet size distribution from the point of release and size of final solid particles formed. The combination of the two models generates results and parametric trends (mainly the effect of leakage size on the size of particles formed). They are then compared with experimental data available in literatures, and validation is achieved. Finally, the model is used to simulate rapid carbon dioxide expansion from pipeline leakage at supercritical storage conditions. Conclusive evidence shows that at supercritical storage conditions (specifically at 310 K and 150 bar), a pipeline leakage will not produce solid CO₂ micro-particles big enough to form a solid rainout pool.

CHAPTER 1

INTRODUCTION

1.1 Background of Study

Anthropogenic emission of CO₂ is becoming a dominant threat to global climate change. In order to mitigate this phenomenon, an approach to capture CO₂ from fossil fuel-using sources, and to store it in natural occurring reservoirs, is suggested. This approach is known as carbon capture and storage (CCS), and the ultimate aim is to capture CO₂ by-product from sources such as industrial processes, power production and fuel decarbonization for preservall and isolation (Herzog & Golomb, 2004).

One of the important aspects in carbon sequestration lies in the transportation of CO₂ to a storage site after the capture process. Transporting CO₂ at a high-pressure, supercritical¹ phase is considered to be the most economically feasible, primarily because the existence of CO₂ as a dense-phase fluid (supercritical) will reduce the risk of sudden phase change. By maintaining a single-phase flow in CO₂ pipelines, operators can avoid abrupt pressure drops and have fewer intermediate boosting stations (Serpa, Morbee, & Tzimas, 2011). From a pipeline integrity point of view, the water solubility limit in CO₂ is found to be 5000 ppm at 75°C and 2000 ppm at 30°C (both are supercritical temperatures). Consequentially, the corrosion rate of carbon steel in dry supercritical CO₂ will be low (Metz, 2005).

Nevertheless, CO₂ transport pipelines can be susceptible to fractures and leakages, which will cause accidental releases of carbon dioxide to the atmosphere (**Figure 1**). Apart from dispersing toxic vapor cloud, this adiabatic expansion of supercritical CO₂

¹ Supercritical carbon dioxide behaves as a supercritical fluid above its critical temperature (31.1°C) and critical pressure (73.9 bar). It expands to fill its container like a gas but has a density like that of a liquid.

will also produce solid CO₂ micro-particles, which - at sizes larger than 100 μm - can rain out to form a solid pool. This rainout pool will eventually evaporate and sublimate to the atmosphere, and contribute significantly to the concentration and dispersion of toxic vapor cloud. When high concentration of CO₂ vapor cloud is dispersed to areas inhabited by human beings, animals and other living things, it will cause severe poisoning and even death. Therefore, it is vital to perform rigorous risk assessment on CO₂ transport pipelines which will pass through populated areas.

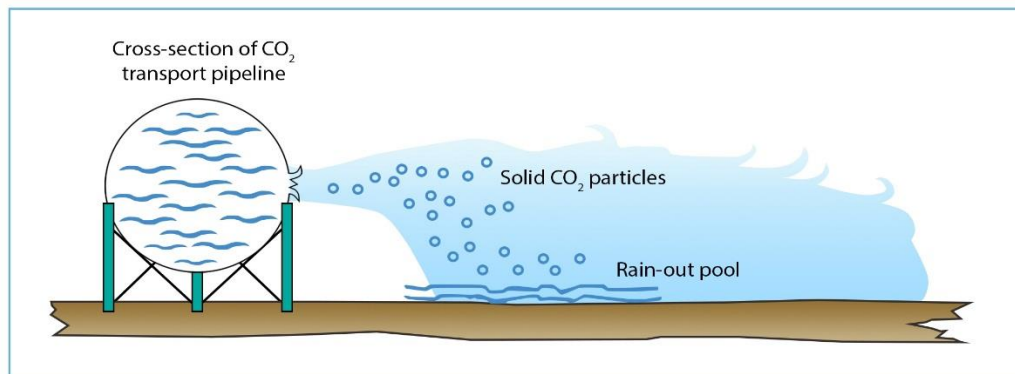


Figure 1: Rapid gas expansion of carbon dioxide

Safety distance quantitatively represents the results of risk assessment performed on the construction and operation of CO₂ transport pipeline. It is defined as the distance from the pipeline where accidental releases will be unable to inflict any intolerable risk on human lives. The key parameters to evaluate safety distance are the concentration and dispersion of CO₂ vapor cloud; in turn, this concentration and dispersion can be greatly affected by the existence of a solid rainout pool. If the existence of the pool is neglected, the concentration and dispersion of CO₂ vapor cloud cannot be calculated correctly, and severe inaccuracy to the safety distance assessment can occur.

Nevertheless, information of solid rainout pool formation in varying discharge scenarios is almost non-existent. It is mainly due to the limited experimental works and modeling techniques that can be used to investigate droplet size distribution and solid particle formation, parameters that will decide the formation of rainout pool. This paper aims to fill these knowledge gaps and enhance the accuracy of risk assessment on CO₂ transport pipelines.

1.2 Problem Statement

While the study of CO₂ vapor cloud dispersion is extensive, most authors choose to neglect the factor of solid pool formation solely based on theories and assumptions (Witlox, Harper, & Oke, 2009; Mazzoldi, Hill, & Colls). It is important, however, to scientifically and quantitatively investigate the size of solid CO₂ micro-particles formed, and determine the subsequent occurrence of a solid rainout pool. Nevertheless, due to the limited study on rapid CO₂ expansion, little information can be extracted from available literatures over the years. Finally, one of the first and most significant experimental works on rapid CO₂ expansion is conducted by Liu, Calvert, Hare, Ghadiri, & Matsusaka in 2012, but there seem to be no available model that can accurately emulate the said process. If a valid model can be constructed based on Liu's experimental findings, the aforementioned problem will be successfully resolved.

1.3 Objective and Scope of Study

The main objective of this paper is to construct a model that can accurately describe rapid CO₂ expansion through an orifice at supercritical storage conditions. The direct results that can be extracted from the model include (1) CO₂ droplet size distribution from the point of release and (2) size of solid CO₂ particles formed.

Below is a list of goals or scope of study that need to be achieved:

1. Model to predict CO₂ droplet size distribution from point of release
2. Model to predict the size of solid CO₂ particles formed
3. To investigate the effect of orifice size on parameters (1) and (2)
4. To validate the obtained results and trends with experimental data published by Liu et al. (2012) and several other literature sources
5. To investigate CO₂ discharge at supercritical storage conditions using validated model

1.4 Relevancy and Feasibility of the Project

The model can accurately describe rapid CO₂ expansion through an orifice at supercritical storage conditions and provide insight on the occurrence of solid CO₂ rainout pool, which are all highly sought-after information required to perform reliable risk assessment on CO₂ transport pipelines. An accurate safety distance of CCS facilities can be obtained to ensure the well-being of humans, animals and other living things.

To ensure the feasibility of the project, the model is constructed by integrating two sub-models: (1) a 3-dimensional Computational Fluid Dynamics (CFD) model, and (2) a mathematical model published by authors Hulsbosch-Dam, Spruijt, Necci & Cozzani (2012). The CFD model functions to obtain temperature and velocity profiles of rapid fluid expansion, while the mathematical model calculates the droplet size distribution from the point of release and size of final solid particles formed. By splitting the model into two major parts, the computational time can be greatly reduced, ensuring the completion of the project within the given timeframe.

For the CFD model, the software FLUENT 14.0 is employed due the fact that it is the most widely used CFD modeling software for a wide range of industrial applications (Sabatino et al., 2007).

CHAPTER 2

LITERATURE REVIEW

In their study, Witlox, Stene, Harper, & Nilsen (2011) developed a model to study the influence of pressure, temperature and orifice size on the mass flow rate of CO₂ release. Their findings are as followed: the flow rate of CO₂ jet increases with increasing pressure, decreases with increasing storage temperature, and increases with increasing orifice size. The model is validated by Witlox (2012) in his review of experimental discharge and dispersion of high-pressure supercritical CO₂ releases. Even though the model is found to provide less accuracy in its prediction when parameters are closer to critical point, it appears to be robust and presents excellent agreement for steady-state flow rate.

While the report by Witlox (2012) is a credible and relevant literature for pressurized releases of supercritical CO₂, it remains to be the only publicly available source of reference for model validation, and does not comprise the aerodynamic and thermodynamic study of CO₂ jet release. Where high-pressure supercritical CO₂ releases are concerned, published experimental data on solid CO₂ formation and particle size distribution, along with its velocity and the influence of jet direction and momentum, remain elusive.

Hulsbosch-Dam, Spruijt, Necci, & Cozzani (2012) attempted to explain the mechanism of CO₂ solidification using their proposed model. In the paper, theories of jet expansion and solid particles formation and rain-out are discussed in great length. The proposed steps are as followed: when the two-phase supercritical fluid is released through the orifice, the liquid droplets in the fluid experience aerodynamic break-up upon exposure to ambient temperature and pressure. Also known as mechanical break-up, it is a consequence of the susceptibility of the droplet to the disturbances imposed

by surrounding vapor flow. Aerodynamic break-up occurs very quickly without any thermal loss, and results in the formation of primary droplets having the same temperature as the released liquid.

Thermodynamic break-up, or flashing, ensues, whereby the primary droplets are superheated at ambient pressure. The system is now composed of liquid droplets surrounded by their own pure vapor, and thermal equilibrium is gradually reached by both boiling and evaporation. According to the authors, when above boiling temperature, a bubble develops in each of what are now known as secondary liquid droplets, experiences growth, and eventually blasts its hosts into several smaller and cooler tertiary droplets. Nucleation and blasting will stop as soon as the temperature drops below boiling point. Finally, when droplets are small enough, they will experience evaporation at their external surfaces and a further reduction in temperature. As CO₂ has a solid-vapor equilibrium at ambient pressure, the tertiary droplets will become small, solid particles when temperature drops below -78 °C.

This process is also known as the Joule-Thompson effect.

The model proposed by Hulsbosch-Dam et al. (2012) is validated against the experimental data of CO₂ release at 65 bar discharge pressure obtained by Liu, Maruyama, & Matsusaka (2010) and corresponds well. The model is also proven accurate in simulating the releases of several other fluid, such as propane, butane and water. Nevertheless, currently there are no available experimental data for releases of supercritical CO₂ that can be used to validate the model.

The experimental result published by Liu et al. (2010) is the closest available source of literature that explores the most fundamental of mechanical and thermodynamic aspects in high-pressure CO₂ jet release. However, in their experiment, carbon dioxide was expanded from the nozzle at a primary pressure of 65 bar, which is still below its supercritical pressure. All the same, Liu et al. (2010) have found that the temperature profile across the jet flow varies: at 1 mm from the nozzle outlet ($x = 1$ mm), the temperature was about -80°C; however, at $x = 50$ mm, it increased to -10°C and subsequently to room temperature when $x > 100$ mm. These findings have indicated that the solidification of carbon dioxide occurs in the first few millimeters from the point of release.

Another experimental study conducted by Liu, Calvert, Hare, Ghadiri, & Matsusaka (2012) found that dry ice particles produced from the expansion nozzle experience growth in the jet flow before subsequent sublimation into smaller particles. For the case of nozzle diameter 0.5 mm, dry ice particles increase in size gradually from about 1 micron at $x = 10$ mm to 3 microns at $x = 50$ mm. Since the experiment was conducted using nozzle diameter of 0.1 mm, 0.2 mm and 0.5 mm, the effect of nozzle size on solid particle formation can also be studied. The results showed that as nozzle size increases, the diameter of the solid particles also increases.

With regard to the relationship between particle size distribution and orifice size, both papers agreed that nozzle diameter plays an important role on the velocity and size of solid CO₂ particles. This is in accordance to the observations of Koornneef et al. (2010). Liu et al. (2010) found that with increasing size of the orifice, the velocity of particles decreases, while the size of the particles increases. Liu et al. (2012) found that the process of growth and subsequent sublimation into smaller particles happens more quickly in smaller orifices than in bigger ones.

On the aspect of rainout pool formation, Witlox, Harper, & Oke (2009), with their UDM² dispersion modeling, presumed that generally no rainout will occur in the course of a horizontal jet expansion. Hulsbosch-Dam et al. (2012) share the same finding in their model for the case of a horizontal pressurized supercritical release. The experiment conducted by Liu et al. (2010) and Liu et al. (2012) observed no rainout as well. The authors agree that rainout is only likely in the case of large orifice size, whereby big solid CO₂ particles (100 – 200 μ m) can be formed.

² Unified dispersion model for jet dispersion, part of consequence modeling package Phast (version 6.53.1)

CHAPTER 3

THEORY

Due to the limited resources available on ANSYS Fluent, running CFD simulations that include the behavior of solid CO₂ particles will consume a huge amount of time. In order to maintain the feasibility of the project, the CFD model is used only to obtain temperature and velocity profiles of the discharge, while the nature of solid CO₂ formation will be mathematically modelled using spreadsheet. The theory proposed by Hulsbosch-Dam et al. (2012) mathematically describes the formation of solid particles during high-pressure CO₂ release as the jet reaches thermal equilibrium.

The theory is in accordance to the Joule-Thompson effect. When carbon dioxide fluid is released from a small orifice, the particles will expand adiabatically and assume a bigger volume. This results in an increased of distance between fluid molecules. The distance between molecules strengthen their intermolecular attractive forces (Van der Waals forces of attraction), and cause an increase in potential energy. Since there is no exchange of heat between the molecules and their surroundings, the gain in potential energy is indicative of a loss in kinetic energy. This means that temperature of the fluid will gradually decrease to reach thermal equilibrium (around -78 °C), which is how solid carbon dioxide particles are formed.

The process can be broken down into three major stages: aerodynamic break-up, thermodynamic break-up, as well as evaporation, solidification and sublimation. It is represented in a diagram shown in **Figure 2**.

3.1 Aerodynamic Break-up

Aerodynamic break-up of CO₂ droplets is isothermal, and can happen within the first few microseconds of the jet release. The author cited Pilch & Erdman (1987) for a correlation between droplet velocity and initial jet velocity with respect to time,

$$\frac{u_d}{u} = \frac{\sqrt{\rho_{vap}}}{\sqrt{\rho_{liq}}} \left(0.5 \cdot \frac{3}{4} \cdot t + 3 \cdot 0.0758 \cdot t^2 \right) \quad (\text{Eq. 1})$$

ρ_{vap} = vapor density

ρ_{liq} = liquid density

The time taken for aerodynamic break-up is determined as the period where there is no temperature increment in the jet. This information can be extracted from the CFD simulation of temperature profile.

The author also assumed that the droplet diameter has a log-normal distribution, citing Razzaghi (1989), and proposed a correlation for average droplet diameter, critical Weber number, surface tension and velocity,

$$D_{av} = \sqrt{\frac{We_{crit}}{\left(1 - \frac{u_d}{u}\right)^2} \frac{\sigma}{\rho_{air} u^2}} \quad (\text{Eq. 2})$$

D_{av} = average particle diameter

We_{crit} = critical Weber number, suggested to be 17 to 18 by Kolev (1993)

σ = liquid surface tension

ρ_{air} = air density

The average diameter obtained is then used in the second part of the manual calculation.

3.2 Thermodynamic Break-up

Thermodynamic break-up of CO₂ droplets includes nucleation, bubble growth and blasting. The calculations can be divided into three main steps in a cycle.

1. Nucleation and bubble growth are the first steps of thermodynamic break-up. The droplet outside radius growth rate is based on an equation by Shusser & Weihs (1999),

$$\frac{dR}{dt} = \left(\frac{2}{3} \frac{\dot{Q}}{\rho_{liq}} \frac{\mathfrak{R}}{M} T_{sat} \right)^{\frac{1}{3}} \quad (\text{Eq. 3})$$

dR_1/dt = rate of droplet radial growth

\dot{Q} = maximum evaporation flux

\mathfrak{R} = gas constant

M = molar weight of carbon dioxide

T_{sat} = equilibrium temperature with the outside temperature

The authors cited the Hertz & Knudsen formula to calculate maximum evaporation flux,

$$\dot{Q} = P_{sat}^* \sqrt{\frac{M}{2\pi\mathfrak{R}T_{sat}}} \quad (\text{Eq. 4})$$

P_{sat}^* = saturated vapor pressure (based on CFD temperature profile)

Once the radial growth rate is obtained, the time taken for the primary droplet to grow until twice its original size is calculated. Distance of this secondary droplet from the point of release can then be calculated based on the velocity profile obtained from the CFD simulation. This information is recorded as part of the particle size distribution data.

2. Blasting or bursting occurs when the outside radius of the droplet reaches two to five times its original size (Vandroux-Koenig and Berhoud, 1997). The value 2 is used, as mentioned in the final part of step 1.

When the primary droplet grows twice its size (value 2 is reached) into secondary droplet, it will blast into several pieces, forming tertiary droplets. The number of resulting droplets can be anything between 1 and 10. A random number generator is used to generate the random number manually. These tertiary droplets will have similar volumes.

3. The final step of this cycle is to test the ability of these tertiary droplets to reboil and nucleate. The authors cited Razzaghi (1989) to calculate a minimum boiling temperature based on particle diameter,

$$T_{min} = T_{boil} \left(1 + \frac{1}{L_v M \rho_{vap}} \frac{4\sigma}{D} \right) \quad (\text{Eq. 5})$$

T_{boil} = bulk boiling temperature

L_v = latent heat of vaporization

If the bulk temperature of the jet at that point is higher than T_{min} , the tertiary droplets will boil, and it is to repeat steps 1 to 3. If the bulk temperature is less than T_{min} , the droplets will proceed to the final stage, which is evaporation, solidification and sublimation.

3.3 Evaporation, Solidification and Sublimation

The final diameter of solid CO₂ particles after the effect of evaporation, solidification and sublimation can be calculated as followed:

$$D_f = \left[D_{in}^3 \frac{\rho_l(T_{in})}{\rho_s(T_{boil})} \frac{[C_{p,l}(T_{in}-T_{tp})-L_v(T_{tp})-C_{p,v}(T_{boil}-T_{tp})]}{[(C_{p,s}-C_{p,v})(T_{boil}-T_{tp})-L_s(T_{tp})-L_v(T_{tp})]} \right]^{\frac{1}{3}} \quad (\text{Eq. 6})$$

T_{in} = initial temperature

T_{boil} = boiling temperature at atmospheric pressure

T_{tp} = triple point temperature

$C_{p,v}$ = specific heat of vapor

$C_{p,l}$ = specific heat of liquid

$C_{p,s}$ = specific heat of solid

L_s = latent heat of solidification

3.4 Graphical Representation of the Three Stages of Solid CO₂ Formation

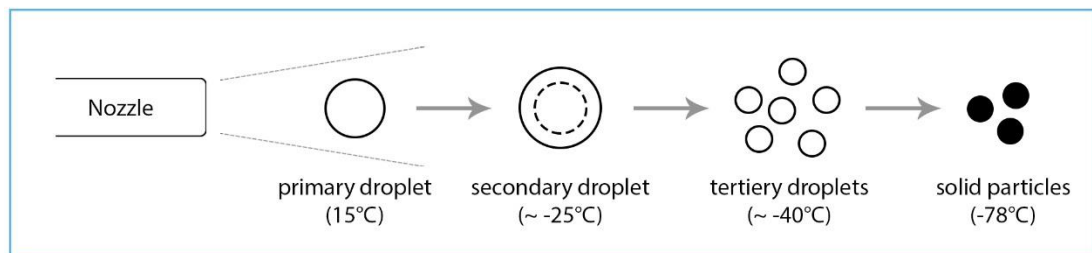


Figure 2: Process of solid particles formation from liquid droplets

CHAPTER 4

RESEARCH METHODOLOGY

4.1 Project Activities

The energy equation and realizable k- ϵ turbulence model are chosen for CFD modeling of turbulent free jet (Molag & Dam, 2011 and Hulsbosch- Dam et al., 2012). Mathematical functions for droplet and particle size calculation are based on model by Hulsbosch-Dam, Spruijt, Necci, & Cozzani (2012).



Analyze and develop the physical geometry based on the experiment conducted by Liu, Calvert, Hare, Ghadiri, & Matsusaka (2012). The boundary condition inputs are also obtained from the same source.



Run CFD simulation on FLUENT until the solution converges. Obtain temperature and velocity profiles. Information is used for calculation of droplet size distribution and size of solid particles formed. Perform parametric study.



Compile available data. Validate results and trends obtained from the model against experimental data obtained from literatures.



Run model at supercritical storage conditions of CO₂ and observe data. Analyze if solid rainout pool will form. For future work, compare data with results obtained by experimental work.

4.2 Boundary Conditions

The boundary conditions of the CFD simulation is based on the experimental design and setup by Liu, Calvert, Hare, Ghadiri, & Matsusaka (2012). Their published result remains the most significant literature that discusses the relationship between particle diameter size and distance from the release orifice, along with information such as effect of varying orifice size and the formation of rainout pool. Below (**Figure 3** and **4**) is the schematic diagram of the authors' experimental apparatus:

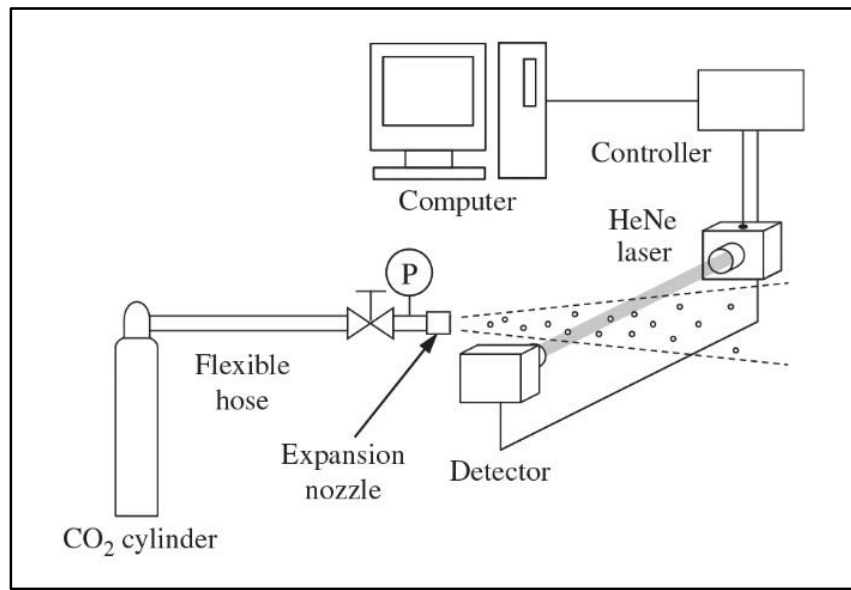


Figure 3: Schematic diagram of Liu et al. (2012) experimental apparatus

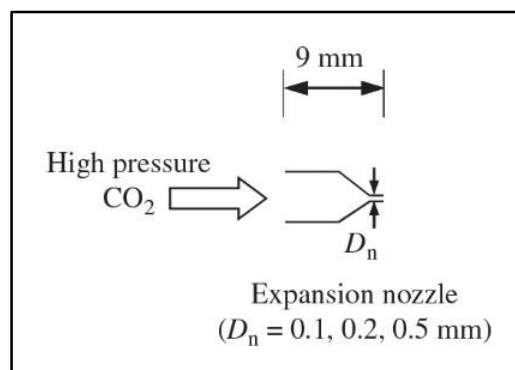


Figure 4: Cross-section of an expansion nozzle

Carbon dioxide is expanded from a nozzle at an upstream pressure of **55 bar** to ambient temperature and pressure (288 K; 101.325 kPa). The detail of the run is described as followed:

Release category: Continuous release
Nozzle diameter: 0.1 mm, 0.2 mm, and 0.5 mm
Duration of release: Immaterial (steady-state)
Wind speed: -
Temperature of fluid: Equilibrium at 195 K

Information that are unavailable in the published literature are acquired by running Aspen HYSYS simulations:

Surface tension: 21.86 dyn/cm (liquid carbon dioxide in air)
Release temperature: 288 K

For the three trials conducted at different nozzle size (consequentially different mass flow rate), the Sauter mean diameter of the solid particles is provided downwind at $x = 10$ mm, 20 mm, 30 mm, 40 mm, and 50 mm.

4.3 CFD Modeling using FLUENT 14.0

A CFD model is designed to describe the rapid fluid expansion of carbon dioxide. The results of interest are temperature and velocity profiles of CO₂ discharge.

4.3.1 Geometry

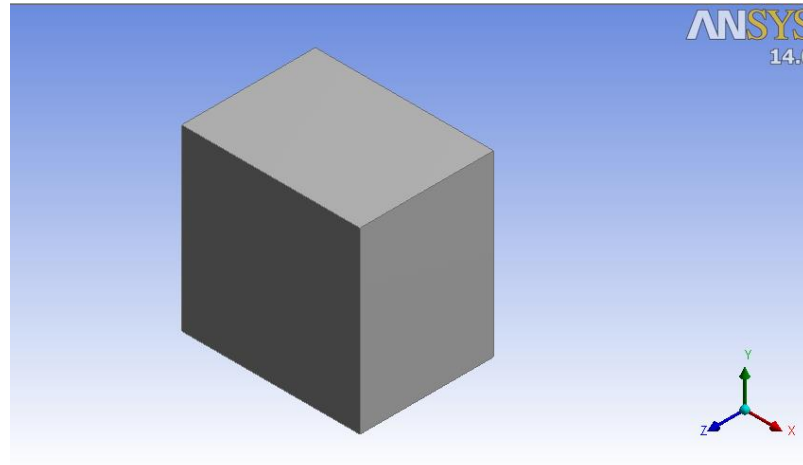


Figure 5: Physical geometry of the CFD simulation

The rectangular geometry in **Figure 5** represents the atmospheric space where CO₂ will be expanded from a nozzle. The dimension of the space is constructed at 15 mm \times 20 mm \times 20 mm. The discharge of CO₂ is in the z-direction from coordinate (0,0,0), and the point of release is constructed at diameters 0.1 mm, 0.2 mm and 0.5 mm. **Figure 6** is the 2D representation of CO₂ discharge, whereby the inlet is denoted by the red box:

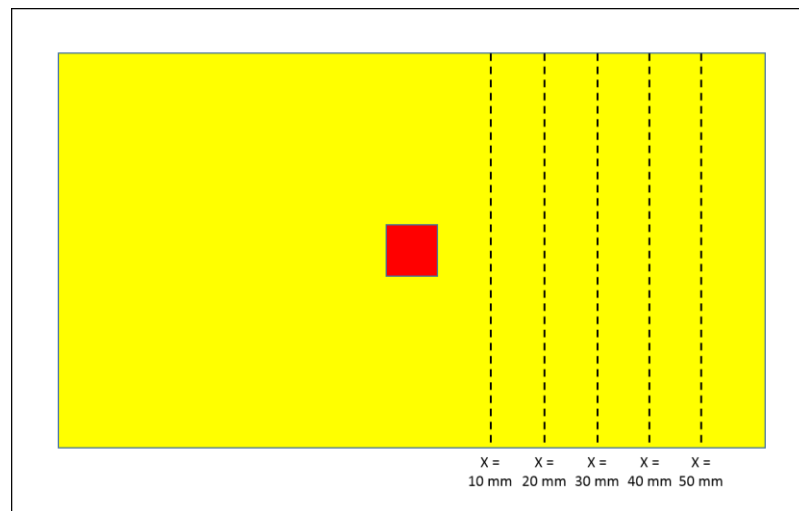


Figure 6: Emulation of experimental layout by Liu et al. (2012) experimental setup

4.3.2 Meshing

The discretization or meshing of the geometry takes the shape of tetrahedral for good quality, and is as followed (**Figure 7** and **8**):

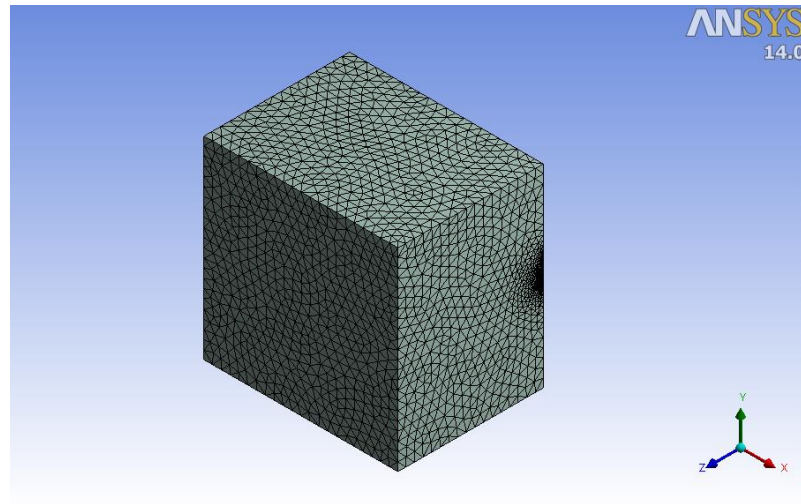


Figure 7: Tetrahedral meshing of geometry

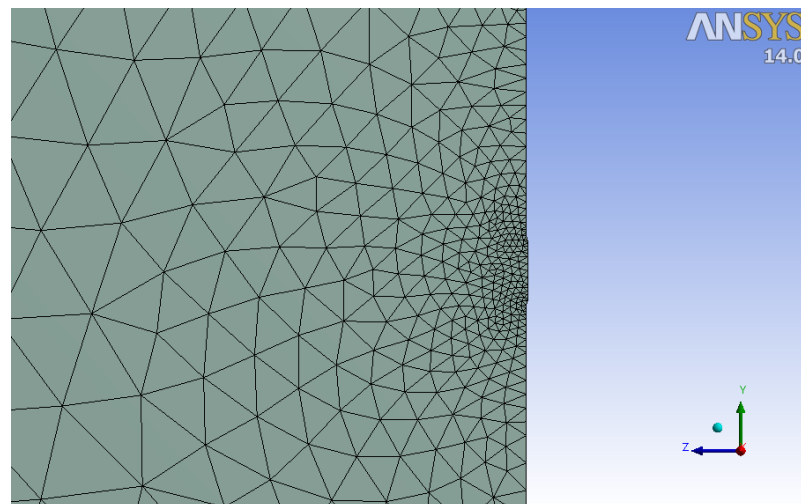


Figure 8: Close-up view of the CO₂ inlet (point of release)

The meshing sizing and statistics are given as followed:

Method:	Tetrahedrons
Min Size:	7.304E-06 m
Max Size:	9.349E-04 m
Growth Rate	1.20
Nodes:	15736
Elements:	83496

4.3.3 Model

The models used for the CFD simulation include the energy equation and the realizable k - ϵ turbulence model. Realizable k - ϵ turbulence model gives an accurate prediction of the spreading rate of both planar and round jets. Various authors (Corina et al., 2011 and Mazzoldi et al., 2011) agreed that these models are suitable to simulate high-pressure CO_2 discharge with solid particle formation. No volume of fluid method is needed for this calculation as the volume fraction of non-vapor (solid particles) is very small.

4.3.4 Materials

The presence of air is negligible due to its low density. The functions proposed by Hulsbosch-Dam et al. (2012) also suggested that there will be no reaction or entrainment of air during CO_2 discharge. Hence, air is not included as one of the materials for this simulation.

The release of CO_2 at 5.5 MPa and 15°C will result in a two-phase flow: vapour and solid. When released to ambient pressure, CO_2 does not form liquid droplets due to its high triple point pressure. Instead, solid CO_2 particles are formed. However, the CFD simulation will assume that the behavior of solid CO_2 particles can be described by the same equations as the behavior of liquid droplets (as far as temperature and velocity profiles are concerned). The physical properties of liquid CO_2 are inserted manually as shown in **Figure 9**.

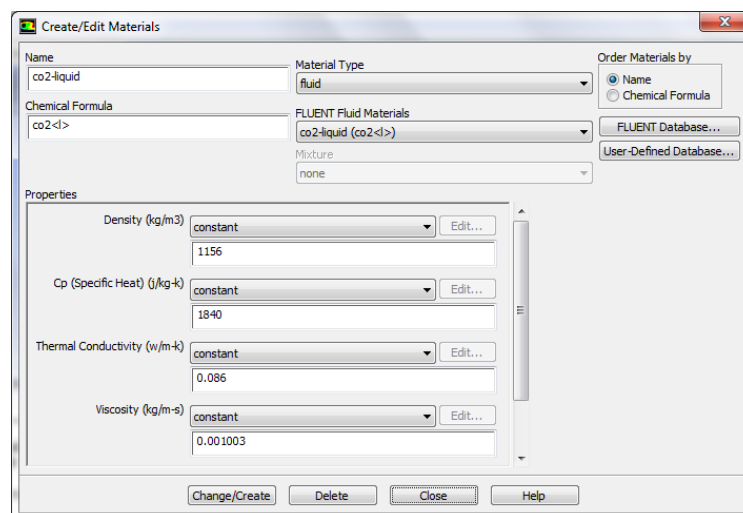


Figure 9: Modification of FLUENT material database

4.3.5 Boundary Conditions

The geometry is halved with a symmetry as both sides are sharing the same activities. The nozzle is set as a mass flow inlet with initial pressure of 55 bar. The mass flow for 0.1 mm, 0.2 mm and 0.5 mm nozzles each has a unique quantity (0.2, 0.5, and 2.9 g/s respectively). The operating pressure of the system is set to be ambient pressure. Pressure outlet is set to have reached saturation temperature 195 K, which is the temperature at which solidification of CO₂ particles is achieved. The temperature and velocity profile can be seen at the symmetry of the setup.

4.3.6 Solution Methods

For this CFD simulation, pressure-based solver and ideal gas fluid properties are used. There is a two-way coupling of mass, momentum, and energy between the particles and the flow. A coupled solver is better than the segregated manner as it is more robust, efficient and superior in performance.

The simulation will iterate until convergence is achieved.

4.4 Mathematical modeling

The core activity is to adapt the mathematical model proposed by Hulsbosch-Dam et al. (2012) and perform calculations and iterations to obtain parameters of interest.

Below (**Figure 10**) is the working flowchart to utilize the mathematical model:

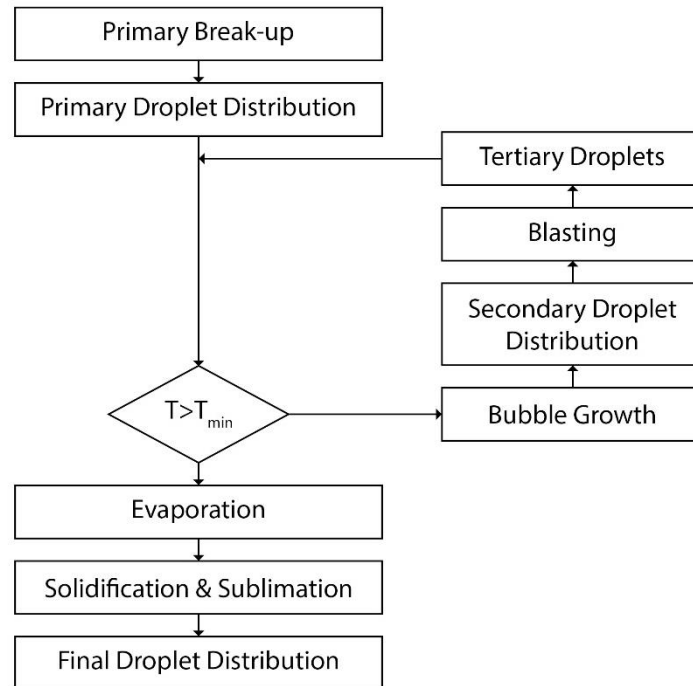
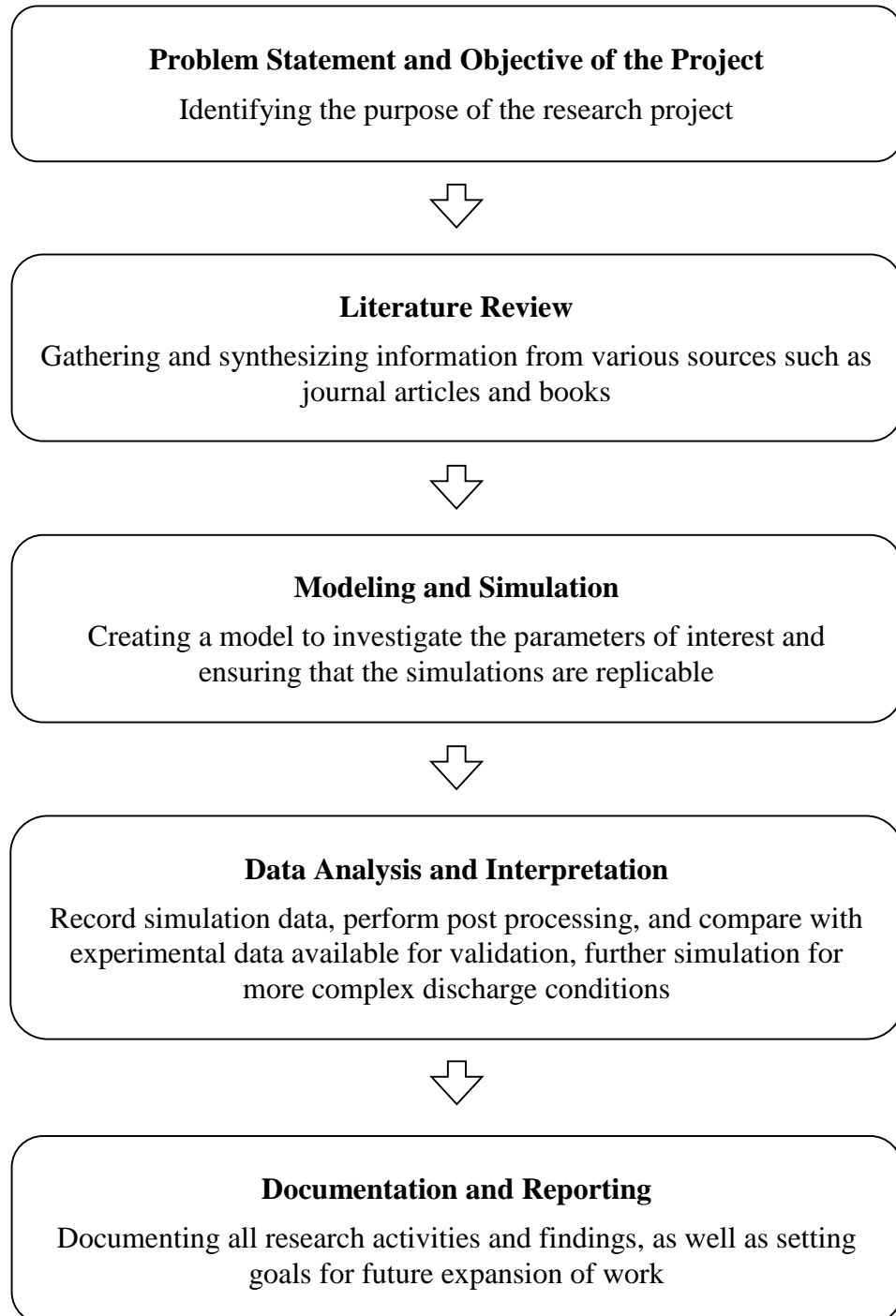


Figure 10: Flow chart of mathematical model

4.5 Key Milestones

Several key milestones must be achieved in order to meet the objective and goals of this project:



4.6 Gantt Chart

Project activities	Week No																											
	1	2	3	4	5	6	7	8	9	10	11	12	13	14	15	16	17	18	19	20	21	22	23	24	25	26	27	28
Selection of project topic																												
Preliminary research work																												
Submission of extended proposal																												
Proposal defence																												
Fine-tuning research methodology																												
Submission of interim draft report																												
Submission of interim report																												
CFD simulation runs																												
Submission of progress report																												
Data post-processing																												
Data analysis and documentation																												
Pre-SEDEX																												
Submission of draft report																												
Submission of dissertation																												
Submission of technical paper																												
Oral presentation																												
Submission of project dissertation																												

•	Milestone
	Process

CHAPTER 5

RESULTS AND DISCUSSION

5.1 CFD Simulation

A simulation with diameter 0.5 mm point of release is carried out as a replicable basis for all other simulations with varying parameters. It is run until convergence is reached. The scaled residuals defined by velocity and turbulence equations decrease to 10^{-3} while the one defined by the energy equation decreases to 10^{-6} . The simulation, which is said to have met the criteria for convergence, is represented as followed (**Figure 11**):

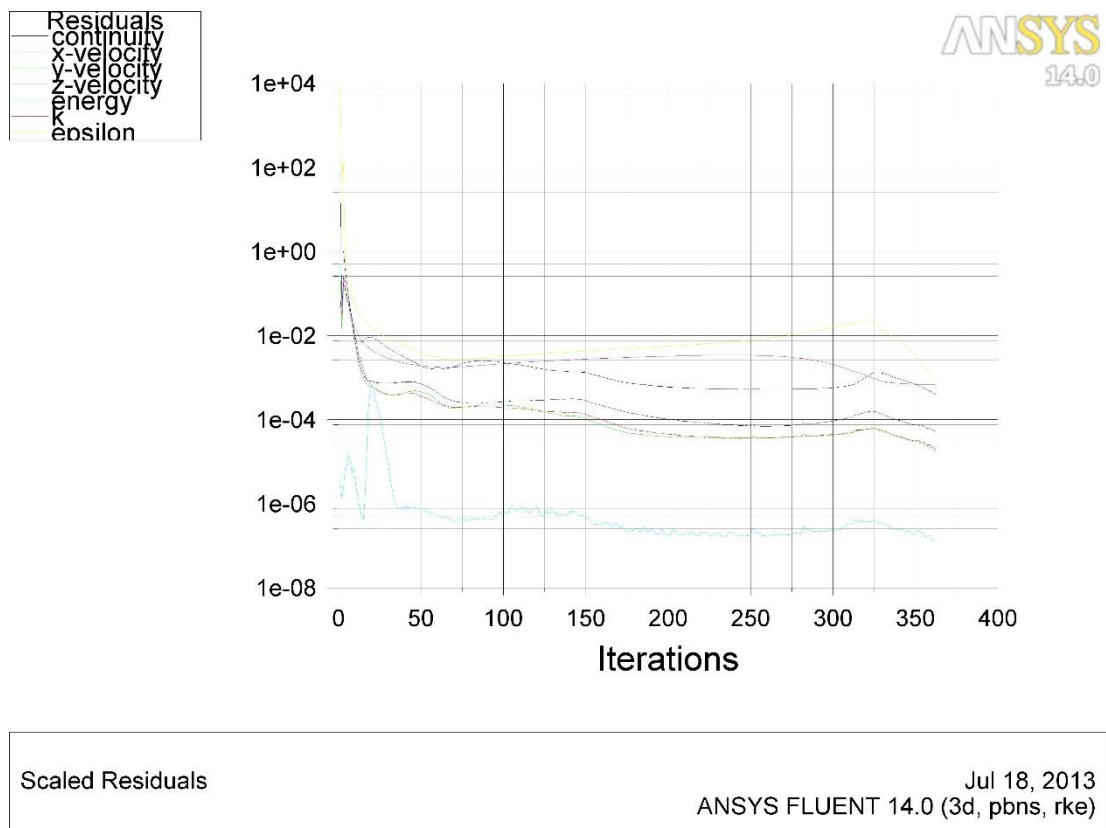


Figure 11: Scaled residuals plot for 360 iterations

The temperature profile contour obtained from the simulation as shown in **Figure 12**:

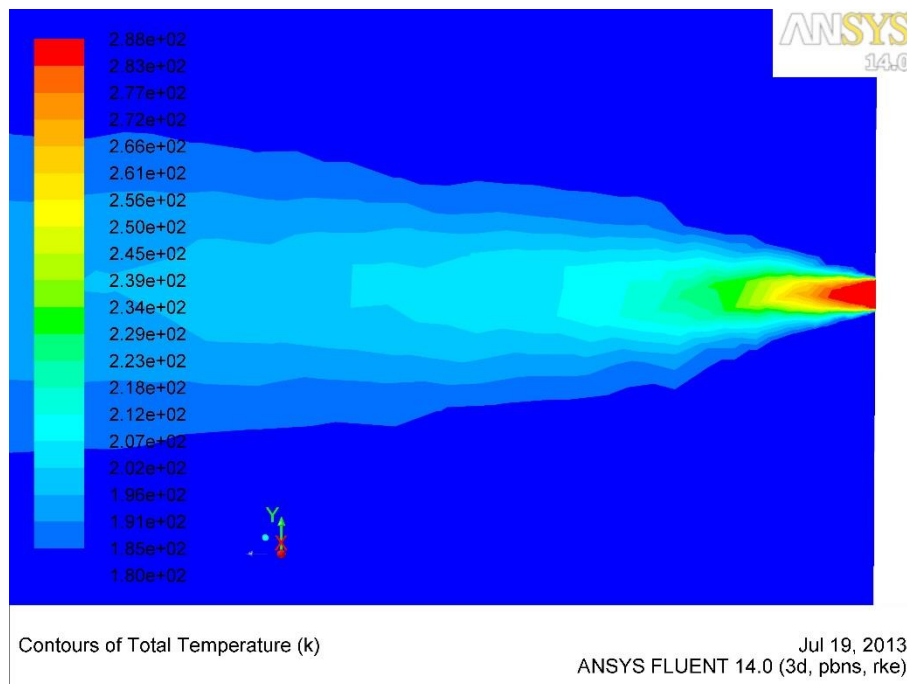


Figure 12: Temperature contours of CO₂ discharge at the point of release

The X-Y plot of temperature profile obtained from the simulation in **Figure 13**:

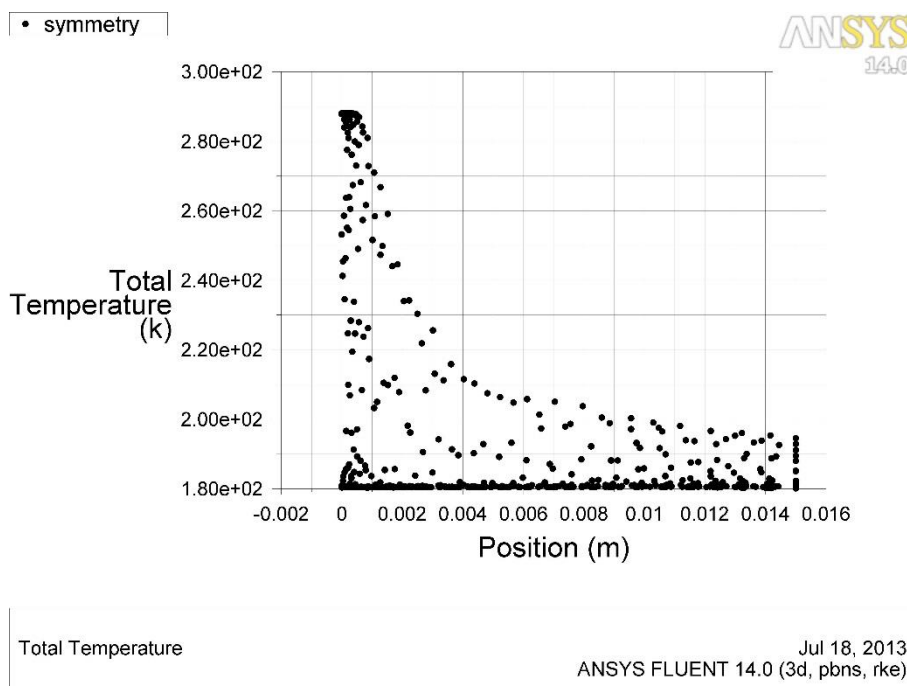


Figure 13: X-Y plot of jet temperature vs. distance from point of release

The X-Y plot of velocity profile obtained from the simulation in **Figure 14**:

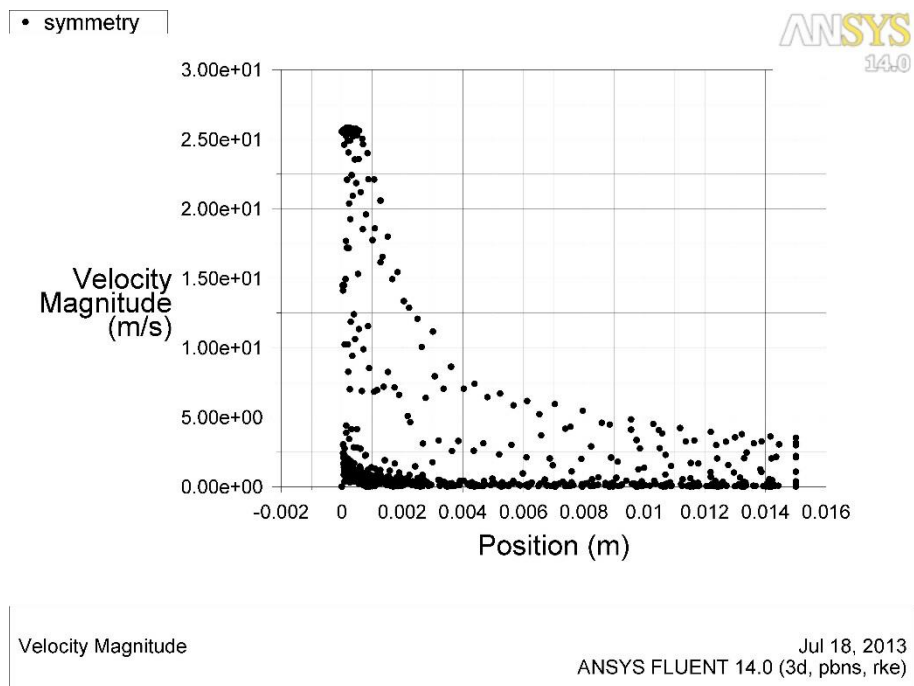


Figure 14: X-Y plot of jet velocity vs. distance from the point of release

The raw X-Y plots obtained directly from Fluent is refined into smooth curves and re-plotted in **Figure 15** and **16**:

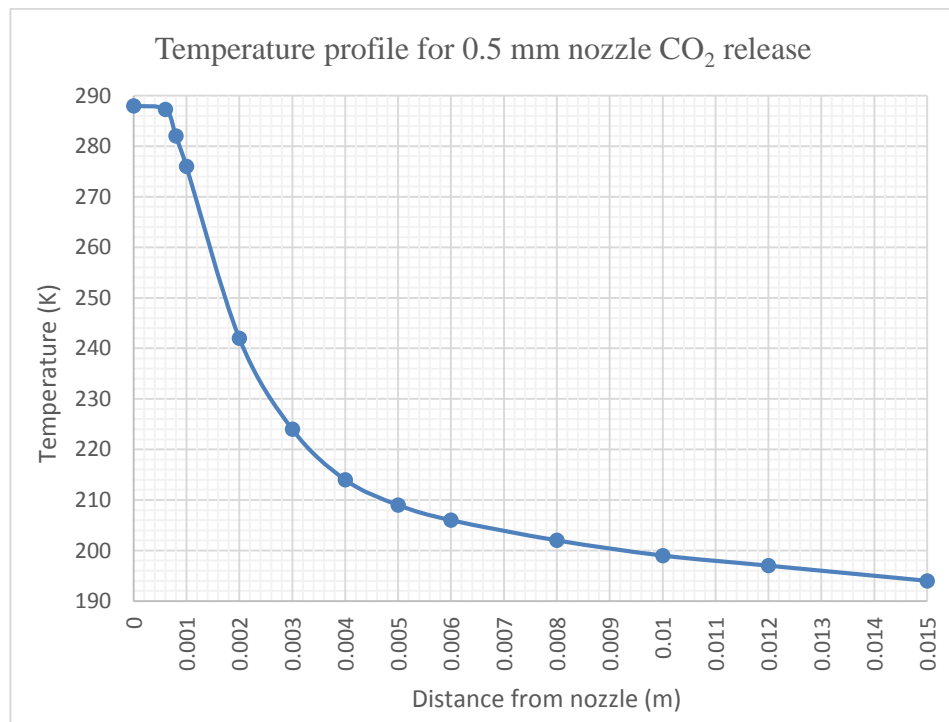


Figure 15: Temperature profile for 0.5 mm nozzle CO₂ release

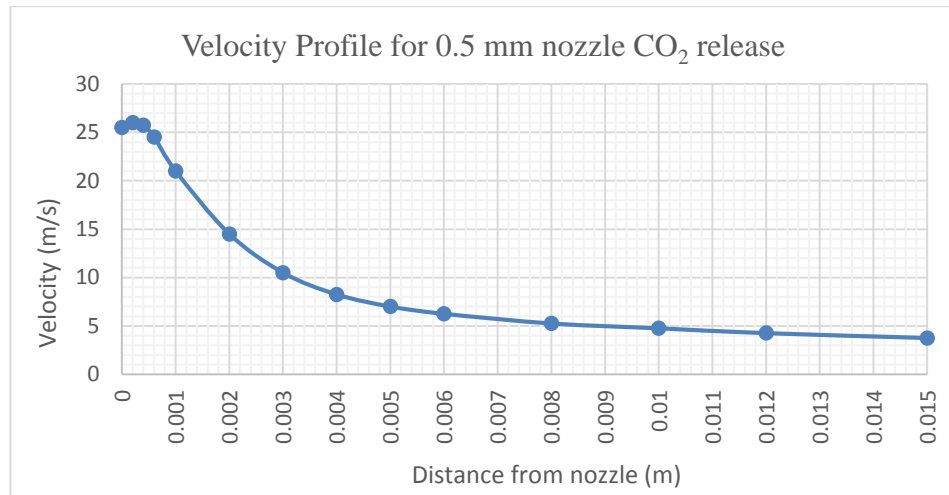


Figure 16: Velocity profile for 0.5 mm nozzle CO₂ release

From **Figure 15**, it can be seen that the bulk temperature decreases as the jet moves away from the nozzle to reach thermal equilibrium. **Figure 16** shows that the CO₂ jet slowly loses its momentum as it moves away from the point of release. The temperature and velocity profiles are used to calculate CO₂ droplet and particle sizes as well as diameter distribution with respect to distance from the point of release.

Keywords:

1. **Droplet:** liquid droplet of CO₂, which can be formed in the first few microseconds of fluid expansion
2. **Particle:** solid particle of CO₂

5.2 Mathematical Calculation

Information about carbon dioxide is collected from literatures and DIPPR database as shown in **Table 1**.

Table 1: Physical properties of carbon dioxide

Saturated temperature, T_{sat} (°C)	194.5
Boiling temperature, T_b (°C)	194.5
Triple point temperature, T_{tp} (°C)	216.4
Surface tension, σ (kg/s ²)	0.02186
Density of air, ρ_{air} (kg/m ³)	1.225
Density of vapor CO ₂ , ρ_{vap} (kg/m ³)	1.7878
Density of liquid CO ₂ , ρ_l (kg/m ³)	1032
Density of solid CO ₂ , ρ_s (kg/m ³)	1562
Critical weber number, We_{crit}	17
Molecular weight of CO ₂ , M	44.01
Gas constant, R (m ³ -Pa/K-mol)	8.314
Latent heat of vaporization, L_v (kJ/kg)	571.08
Latent heat of fusion, L_s (kJ/kg)	196.10
Specific heat of vapour, $C_{p,v}$ (kJ/kg-K)	0.8390
Specific heat of liquid, $C_{p,l}$ (kJ/kg-K)	2.0458
Specific heat of solid, $C_{p,s}$ (kJ/kg-K)	1.1580

5.2.1 Aerodynamic break-up

By referring to the temperature profile in **Figure 15**, the temperature remains the same (isothermal) until it is 0.4 mm away from the point of release ($d = 0.4$ mm). The initial

velocity, u of the fluid expansion is given in **Figure 16** as 25.5 m/s. Time taken for the aerodynamic breakup is then calculated as followed:

$$t = \frac{d}{u} = \frac{0.0004}{25.5} = 1.57 \times 10^{-5} \text{ s}$$

By using **Equation 1**, the droplet velocity is calculated as followed:

$$\begin{aligned} \frac{u_d}{u} &= \frac{\sqrt{\rho_{vap}}}{\sqrt{\rho_{liq}}} \left(0.5 \cdot \frac{3}{4} \cdot t + 3 \cdot 0.0758 \cdot t^2 \right) \\ &= \frac{\sqrt{1.7878}}{\sqrt{1032}} \left[0.5 \cdot \frac{3}{4} \cdot 1.57 \times 10^{-5} + 3 \cdot 0.0758 \cdot (1.57 \times 10^{-5})^2 \right] \\ &= 2.45 \times 10^{-7} \end{aligned}$$

$$u_d = 2.45 \times 10^{-7} \times 25.5 \text{ m/s} = 6.24 \times 10^{-6} \text{ m/s}$$

The average diameter of the droplet is calculated using **Equation 2** as followed:

$$D_{av} = \frac{\sqrt{We_{crit}}}{\left(1 - \frac{u_d}{u}\right)^2} \frac{\sigma}{\rho_{air} u^2} = \frac{\sqrt{17}}{\left(1 - \frac{6.24 \times 10^{-6}}{25.5}\right)^2} \times \frac{0.02186}{1.225(25.5)^2} = 1.132 \times 10^{-4} \text{ m}$$

5.2.2 Thermodynamic break-up

The first step is to check if the bulk temperature of the jet is higher than the minimum temperature at which the droplets will boil. At 0.4 mm from the point of release, **Figure 15** shows that the bulk temperature is at 288 K. The minimum temperature at which the droplets are subjected to boiling is calculated using **Equation 5** as followed:

$$\begin{aligned} T_{min} &= T_{boil} \left(1 + \frac{1}{L_v M \rho_{vap}} \frac{\sigma}{D} \right) = 194.5 \left(1 + \frac{1}{571.08 \times 44.01 \times 1.7878} \times \frac{0.02186}{1.132 \times 10^{-4}} \right) \\ &= 195.34 \text{ K} \end{aligned}$$

As the bulk temperature is higher than the minimum boiling temperature of the droplets, the droplets will begin to nucleate and subsequently boil and blast.

The maximum surface evaporation flux calculated using **Equation 4** as followed:

$$\dot{Q} = P_{sat}^* \sqrt{\frac{M}{2\pi \Re T_{sat}}} = 4500000 \sqrt{\frac{44.01}{2\pi \times 8.314 \times 194.5}} = 296165 \text{ g/m}^2\text{s}$$

Note that vapor pressure is obtained from **Figure 24** (Appendix I) corresponding to the bulk temperature.

The nucleation and bubble radius growth rate is then calculated using **Equation 3** as followed:

$$\frac{dR}{dt} = \left(\frac{2}{3} \frac{\dot{Q}}{\rho_{liq}} \frac{R}{M} T_{sat} \right)^{\frac{1}{3}} = \left(\frac{2}{3} \times \frac{296165}{1032000} \times \frac{8.314}{44.01} \times 194.5 \right)^{\frac{1}{3}} = 1.916 \text{ m/s}$$

The diameter growth rate will be twice that of the radius growth rate, as followed:

$$\frac{dD}{dt} = 3.831 \text{ m/s}$$

Since the initial diameter of the droplet is calculated as 1.132E-04 m, and it will burst when it grows twice its size, the diameter at which it will burst is 2.264E-04 m. Time taken for the droplet to reach blasting can then be calculated as followed:

$$t_{blast} = \frac{2.264 \times 10^{-4} - 1.132 \times 10^{-4}}{3.831} = 2.953 \times 10^{-5} \text{ s}$$

The distance of droplet from point of release before blasting is at 0.4 mm, and the velocity is given as 25.75 m/s (referring to **Figure 16**). The time taken for the droplet to nucleate and blast is given as 29.53 μ s. Therefore, the distance traveled during nucleation and blasting is calculated as followed:

$$\text{Current distance} = \frac{25.75}{2.953 \times 10^{-5}} = 0.76 \text{ mm}$$

The current distance of the droplet from point of release = 0.4 + 0.76 = 1.16 mm.

The droplet is then said to blast into several equal-sized small droplets. The amount of small droplets formed can be any random number between 1 and 10. A random number generator is used to generate 1000 numbers within that range and the median of its cumulative distribution is identified. The number is 4.946. The diameter of the resulting small droplets is then calculated as followed:

$$D_{current} = \frac{2.264 \times 10^{-4}}{4.946} = 4.576 \times 10^{-5} \text{ m}$$

It is now necessary to investigate whether the newly formed droplets are subjected to boiling and blasting. At 45.76 μm in diameter, the droplets will boil if the bulk temperature is higher than 196.57 K (calculated using **Equation 5**). At current distance of 0.76 mm, **Figure 15** tells us that the bulk temperature is at 266 K. Therefore, the entire thermodynamic break-up process will repeat, until bulk temperature is lower than the minimum boiling temperature. This happens after 6 iterations, and the resulting droplets are 1.22 μm in diameter (complete calculation spreadsheet is given in Appendix II).

5.2.3 Evaporation and solidification

When the droplets will no longer boil, it will be subjected to evaporation and subsequent solidification. The final solid particle size is calculated as followed:

$$D_f = \left[D_{in}^3 \frac{\rho_l(T_{in})}{\rho_s(T_{boil})} \frac{[C_{p,l}(T_{in} - T_{tp}) - L_v(T_{tp}) - C_{p,v}(T_{boil} - T_{tp})]}{[(C_{p,s} - C_{p,v})(T_{boil} - T_{tp}) - L_s(T_{tp}) - L_v(T_{tp})]} \right]^{\frac{1}{3}} = 1.048 \mu\text{m}$$

5.3 Model Validation

5.3.1 Validation against experimental findings by Liu et al. (2012)

The CFD simulation and mathematical calculations are repeated for release orifice diameter 0.2 mm and 0.1 mm as to emulate the experimental setup in Liu's research. The complete simulation results and calculation spreadsheets are given in Appendix III. The calculated values are compared with the experimental findings in **Table 2**:

Table 2: Validation of model against Liu et al. (2012)

Nozzle diameter (mm)	Inlet mass flow rate (g/s)	Experimental particle size (μm)	Simulation particle size (μm)	Percentage error (%)
0.5	2.9	1.000	1.048	4.80
0.2	0.5	0.950	0.936	1.52
0.1	0.2	0.900	0.891	1.04

Note: storage temperature and pressure are 288 K and 55 bar respectively

It is found that the error is less than 5%, indicating that the model is sufficiently accurate.

5.3.2 Validation against experimental findings by Liu et al. (2010)

The experiment conducted by Liu and team in 2010 provided only the temperature profile for high-pressure release of carbon dioxide from a 0.2 mm diameter nozzle. The temperature profile is given as followed:

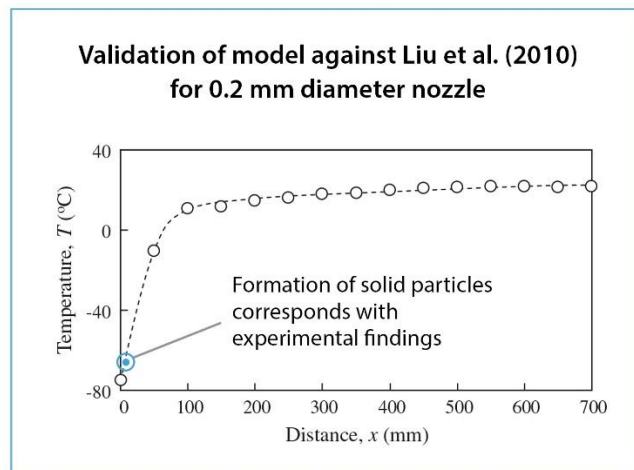


Figure 17: Validation of model against Liu et al. (2010) for 0.2 mm diameter nozzle

Referring to the CFD simulation, for a 0.2 mm diameter nozzle release, solidification of CO₂ droplets into particles occur approximately 7.4 mm away from the point of release (temperature at 195 K or 78 °C). This finding corresponds well with the temperature profile experimentally obtained by Liu et al. (2010), as shown in **Figure 17**, whereby the freezing point of CO₂ is within the first 10 mm from the point of release. It is, again, indicative that the model is sufficiently accurate.

5.4 Parametric Study for Validation of Trends

5.4.1 Effect of Nozzle Diameter on Droplet Size Distribution and Particle Size Formation

The model is used to investigate the effect of nozzle diameter, and therefore a range of nozzle size between 0.1 and 0.5 mm diameter is set (CFD simulations and calculation spreadsheets are available in Appendix III). The following charts summarize the findings:

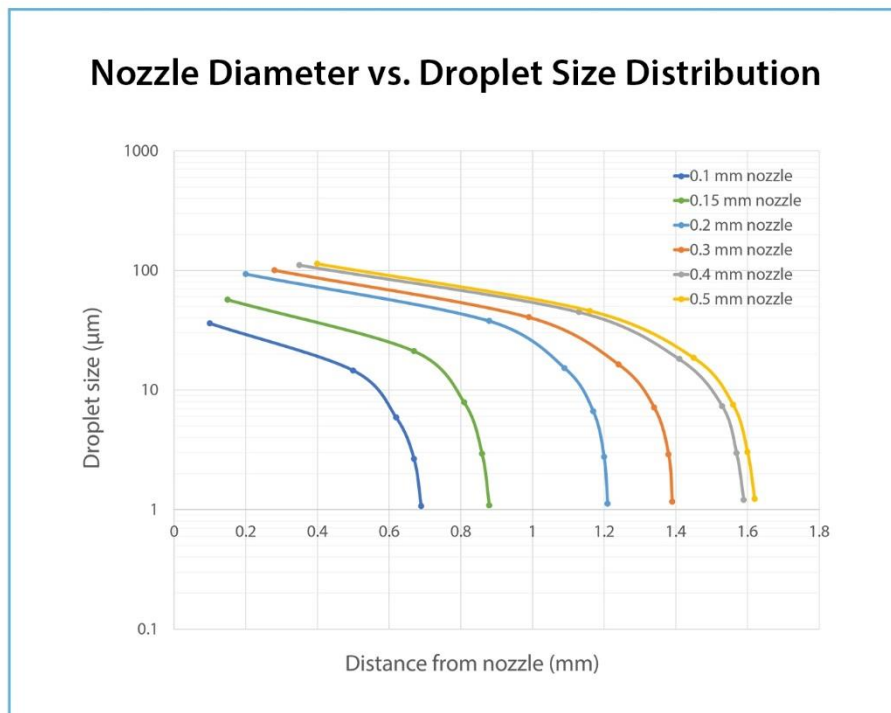


Figure 18: Effect of nozzle diameter on droplet size distribution

From **Figure 18** it can be seen that the carbon dioxide droplets reduce in size log-normally as they travel away from the point of release. It is also observed that cooling,

evaporation and sublimation occur more quickly in smaller orifices than in bigger one. It requires a longer time for the droplets to reach terminal small sizes (~ 1 micron) when carbon dioxide is expanded from a bigger orifice compared to a smaller one. **Figure 19** shows that the final solid particles formed increase in size as the orifice size increases.

The abovementioned trends are all in accordance to the research conducted by Witlox et al. (2009), Liu et al. (2012), and Hulsbosch-Dam et al. (2012). This warrants the relevance, reliability and replicability of the model.

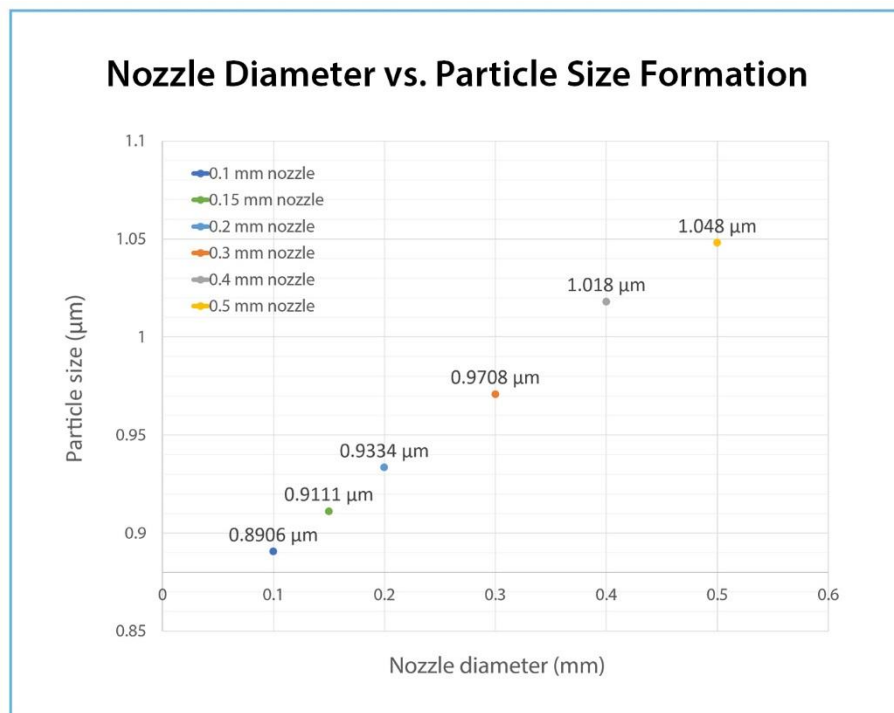


Figure 19: Effect of nozzle diameter on particle size formation

5.5 Supercritical Release

In carbon capture and storage (CCS) technology, carbon dioxide is usually transported at supercritical conditions for higher efficiency. Therefore, it is of interest to investigate the fluid expansion phenomenon in the case of a pipeline leakage at supercritical carbon dioxide transport pipeline. Witlox (2012) suggests a range of industrial storage pressure for the investigation, which is between 100 to 150 bar. A pressure of 150 bar is used, for leakage (orifice) diameter between 0.1 mm to 2 mm. The CFD simulations and calculation spreadsheets are attached in Appendix IV. The results obtained are shown in **Figure 20**.

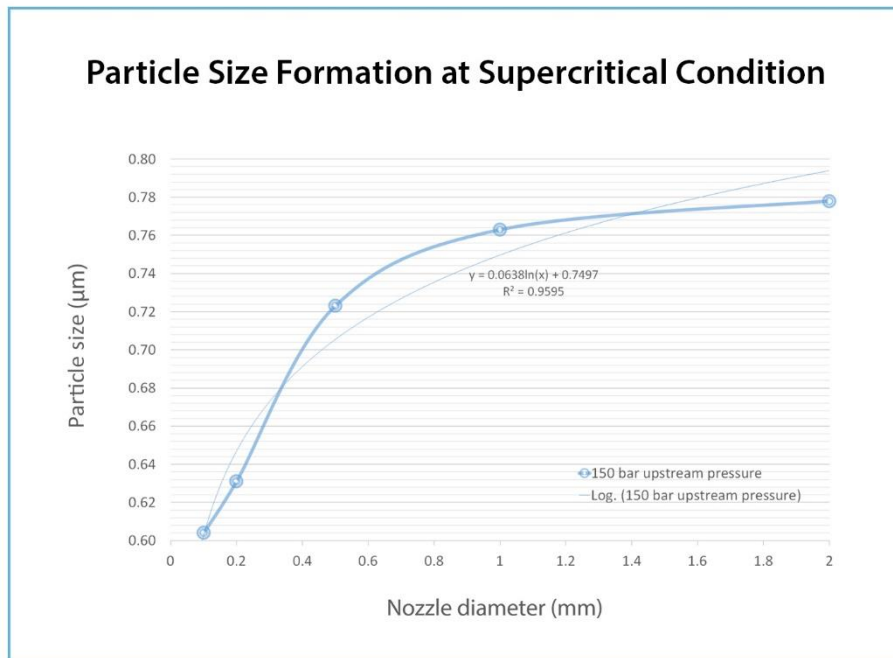


Figure 20: Particle size formation at supercritical storage condition (310 K and 150 bar)

It shows that the range of solid particles formed are between 0.6 and 0.8 μm . The solid particles formed are smaller in size when the storage pressure is higher (150 bar) compared to the case when the storage pressure is lower (55 bar). This finding corresponds to the study by Witlox et al. (2009), which demonstrated that bigger solid particles were formed when the storage pressure was lower.

It is also highly of interest whether or not solid particles formed during supercritical releases will subsequently form a rainout pool. As shown in **Figure 20**, the increment in solid particle size can be seen as logarithmic when nozzle diameter increases. With a regression of 0.9595, the relationship can be equated as followed:

$$y = 0.0638 \ln(x) + 0.7497 \quad (\text{Eq. 7})$$

According to Hulsbosch-Dam et al. (2012), in the case of horizontal releases, rainout pool will only form when the solid particles formed are at least 100 μm in diameter. Using **Equation 7**, rudimentarily, it is found that in order for the solid particles to reach the size of 100 μm , the diameter of the leakage (orifice) will have to be infinite. To further visualise, for a big leakage of 20 mm in diameter, the solid particles formed only assume a diameter of 0.94 μm , not significantly big enough to cause a rainout pool formation. Therefore, for CO_2 releases with supercritical storage condition (specifically at 150 bar), there will be no rainout pool formation.

By applying the above technique, researchers can use storage pressure, temperature and orifice diameter as manipulative variables to investigate whether or not the formation of a rainout pool can be ignored, and accurately predict the dispersion of carbon dioxide in the case of an accidental pipeline leakage.

CHAPTER 6

CONCLUSION

All the goals or research activities set for the project are completed, and the objective is successfully achieved. A model is successfully constructed to investigate the rapid expansion of carbon dioxide through a nozzle. It is able to accurately predict the CO₂ droplet size distribution from point of release, as well as the size of solid particle formed. The model is also validated by several sources of literature in terms of results (direct calculation) and parametric trends. Finally, CO₂ expansion is simulated at supercritical storage conditions (specifically at 310 K and 150 bar) to observe droplet size distribution and size of solid particles formed. It is conclusive that in the course of a horizontal release, particles will only assume the size of less than 1 micron, which makes the formation of a solid rainout pool impossible.

FUTURE WORK AND EXPANSION

Since currently there is no available experimental data on particle diameter size distribution of a supercritical CO₂, it is recommended that an experimental rig is set up in order to fulfill this knowledge gap.

The experimental setup aims to model a high-pressure supercritical CO₂ pipeline and the rapid expansion of CO₂ fluid. We refer to the work of Helfgen, Hils, Holzknacht, Türk, & Schaber (2001), who developed an experimental setup consisting of a solvent cylinder (in our case, a carbon dioxide cylinder), a pump, a heating element, a capillary nozzle (in our case, an expansion nozzle) and necessary piping/tubing. The equipment is arranged in abovementioned order; that is, fluid will be compressed by pump to reach pressure above critical point, followed by the elevation of its temperature to above critical point. For our experimental setup, the heating element is placed before the booster pump so that CO₂ can remain vapor before pressurization, in which case the lifespan of the pump can be prolonged. Below is the schematic:

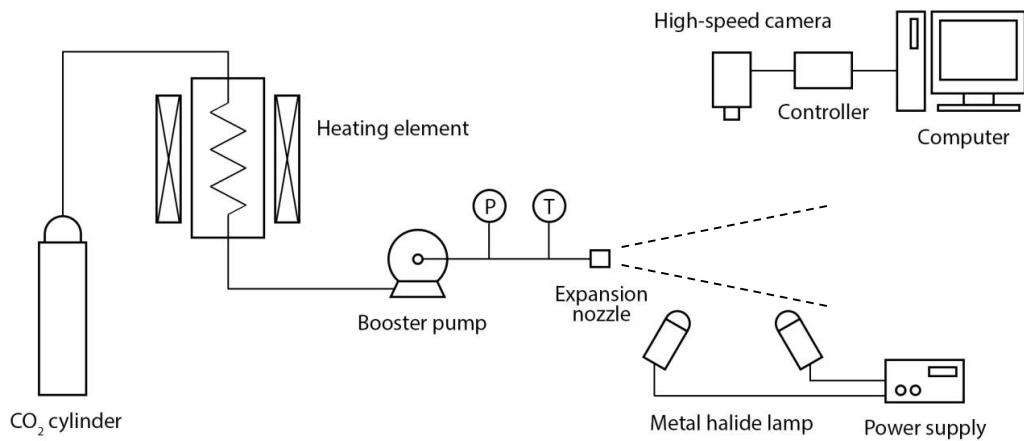


Figure 21: Experimental apparatus and setup

Droplet Velocity and Size Measurement

A microscopic high-speed camera is used with the illumination from metal halide lamps to capture images of CO₂ particles expanding from the nozzle. This technique is known as imaging, and can be used to measure droplet velocity and size by applying Digital Image Analysis (Lad, Aroussi, & Muhamad Said, 2011). Lad et al. (2011) primarily propose calibration techniques that allow post-processing of measured data in order to obtain a more accurate estimate.

To determine velocity of the particles, side view images of the jet expansion are captured for post-processing. Velocity can then be calculated from the length of the trajectories of the dry ice particles. However, there will be a distribution of particle velocities in a single image. Hence median values are located from lognormal graphs of the distribution for perusal.

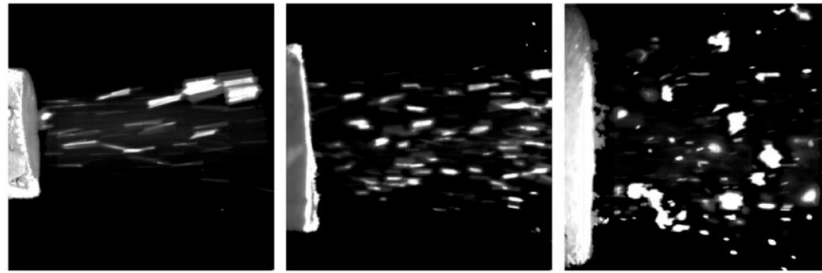


Figure 22: Dry ice particles in jet flow

The size (and shape) of the particles cannot be determined by side view imaging because the particles are moving at high velocities and many are out of focus. Therefore, it is suggested that the images be taken from a glass plate, which is set directly in front of the jet flow. This way, dry ice particles will be trapped on the glass surface and the ones in the same focus depth can be observed with ease. The calculation of the droplet size will be in equivalent diameter.



Figure 23: Dry ice particles trapped on glass surface

Droplet Size Distribution

In order to determine the distribution of particle size over a range of distance from the expansion nozzle, the same techniques as above can be used. Additionally, the distance of glass plate from the expansion nozzle is varied so that particle size at different distances can be measured and tabulated.

CHAPTER 7

REFERENCES

- Herzog, H., & Golomb, D. (2004). Carbon Capture and Storage from Fossil Fuel Use. In J. C. Editor-in-Chief: Cutler (Ed.), *Encyclopedia of Energy* (pp. 277-287). New York: Elsevier.
- Hulsbosch-Dam, C. E. C., Spruijt, M. P. N., Necci, A., & Cozzani, V. (2012). Assessment of particle size distribution in CO₂ accidental releases. *Journal of Loss Prevention in the Process Industries*, 25(2), 254-262. doi: <http://dx.doi.org/10.1016/j.jlp.2011.10.009>
- Koornneef, J., Spruijt, M., Molag, M., Ramírez, A., Turkenburg, W., & Faaij, A. (2010). Quantitative risk assessment of CO₂ transport by pipelines—A review of uncertainties and their impacts. *Journal of Hazardous Materials*, 177(1–3), 12-27. doi: <http://dx.doi.org/10.1016/j.jhazmat.2009.11.068>
- Lad, N., Aroussi, A., & Muhamad Said, M. F. (2011). Droplet Size Measurement for Liquid Spray using Digital Image Analysis Technique. *Journal of Applied Sciences*, 11, 1966-1972. doi: 10.3923/jas.2011.1966.1972
- Liu, Y., Calvert, G., Hare, C., Ghadiri, M., & Matsusaka, S. (2012). Size measurement of dry ice particles produced from liquid carbon dioxide. *Journal of Aerosol Science*, 48(0), 1-9. doi: <http://dx.doi.org/10.1016/j.jaerosci.2012.01.007>
- Liu, Y., Maruyama, H., & Matsusaka, S. (2010). Agglomeration process of dry ice particles produced by expanding liquid carbon dioxide. *Advanced Powder Technology*, 21(6), 652-657. doi: <http://dx.doi.org/10.1016/j.appt.2010.07.009>

- Metz, B. (2005). Carbon Dioxide Capture and Storage: Special Report of the Intergovernmental Panel on Climate Change: Cambridge University Press.
- Molag, M., & Dam, C. (2011). Modelling of accidental releases from a high pressure CO₂ pipelines. *Energy Procedia*, 4(0), 2301-2307. doi: <http://dx.doi.org/10.1016/j.egypro.2011.02.120>
- Sabatino, S. D., Buccolieri, R., Pulvirenti, B., & Britter, R. E. (2007). Flow and Pollutant Dispersion in Street Canyons using FLUENT and ADMS-Urban. *Environmental Model & Assessment*, 369-381.
- Serpa, J., Morbee, J., & Tzimas, E. (2011). Technical and Economic Characteristics of a CO₂ Transmission Pipeline Infrastructure: JRC Scientific and Technical Reports. Luxembourg.
- Witlox, H. W. M. (2012). Data review and Phast analysis (discharge and atmospheric dispersion) for BP DF1 CO₂ experiments. London: Det Norske Veritas Energy.
- Witlox, H. W. M., Harper, M., & Oke, A. (2009). Modelling of discharge and atmospheric dispersion for carbon dioxide releases. *Journal of Loss Prevention in the Process Industries*, 22(6), 795-802. doi: <http://dx.doi.org/10.1016/j.jlp.2009.08.007>
- Witlox, H. W. M., Stene, J., Harper, M., & Nilsen, S. H. (2011). Modelling of discharge and atmospheric dispersion for carbon dioxide releases including sensitivity analysis for wide range of scenarios. *Energy Procedia*, 4(0), 2253-2260. doi: <http://dx.doi.org/10.1016/j.egypro.2011.02.114>

CHAPTER 8

APPENDICES

APPENDIX I

CO₂ VAPOR PRESSURE GRAPH

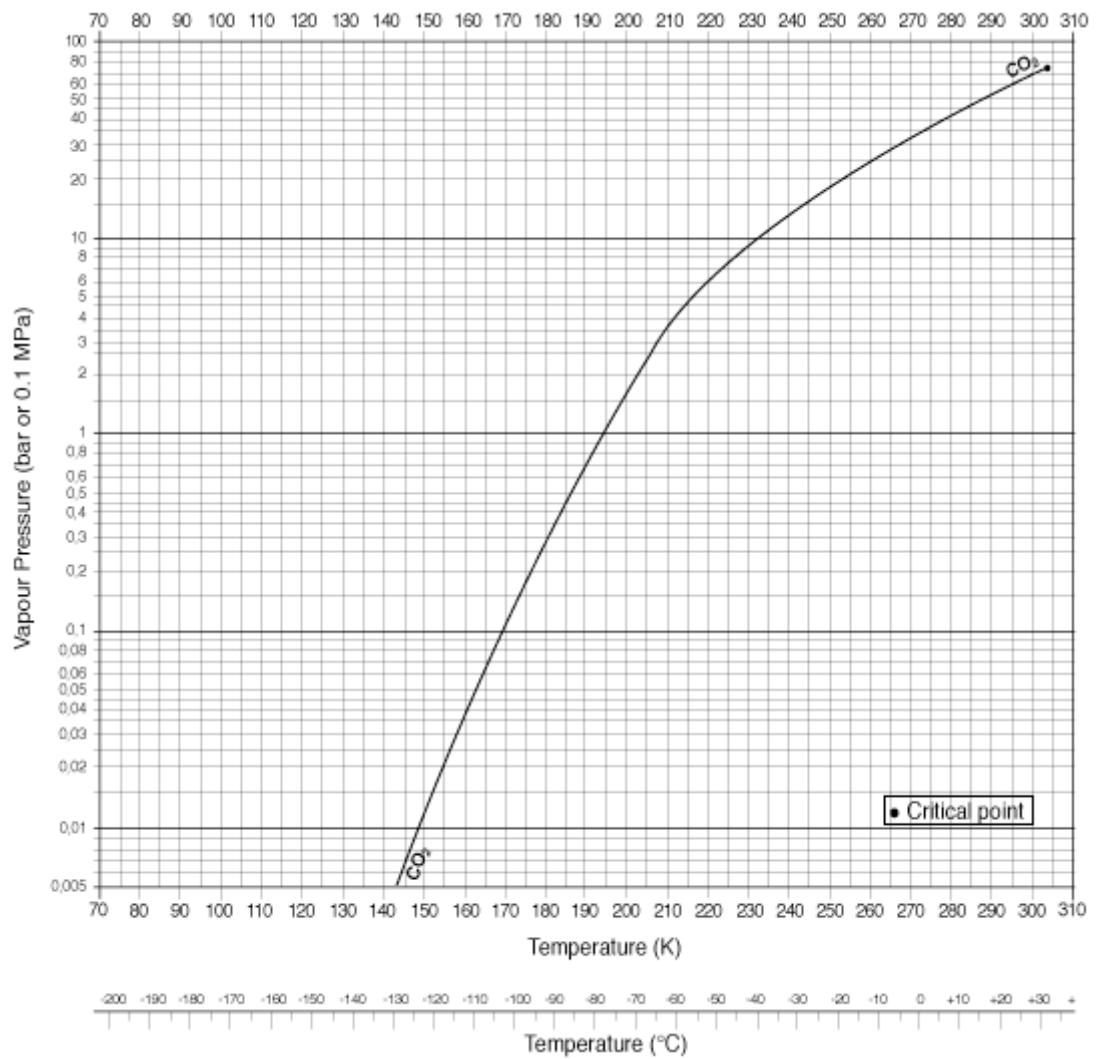


Figure 24: Carbon dioxide vapor pressure graph

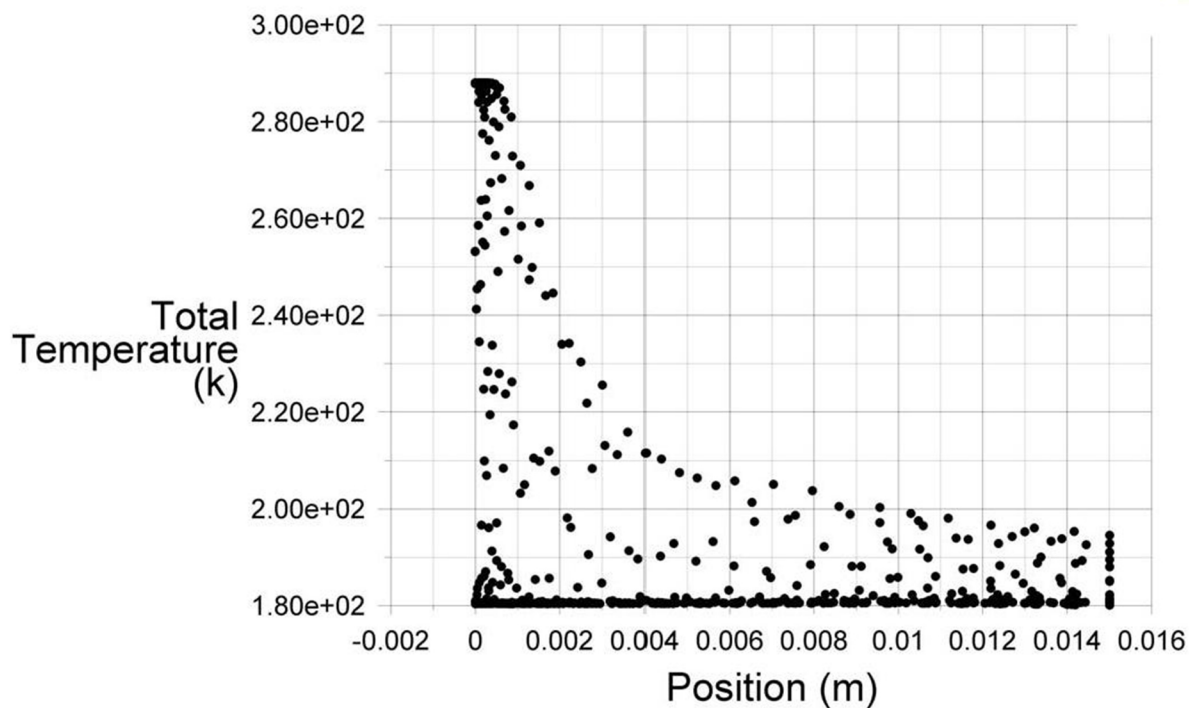
APPENDIX II

CFD SIMULATION AND MATHEMATICAL CALCULATION OF CO₂ EXPANSION THROUGH 0.5 MM DIAMETER NOZZLE

0.5 MM DIAMETER

• symmetry

ANSYS
14.0

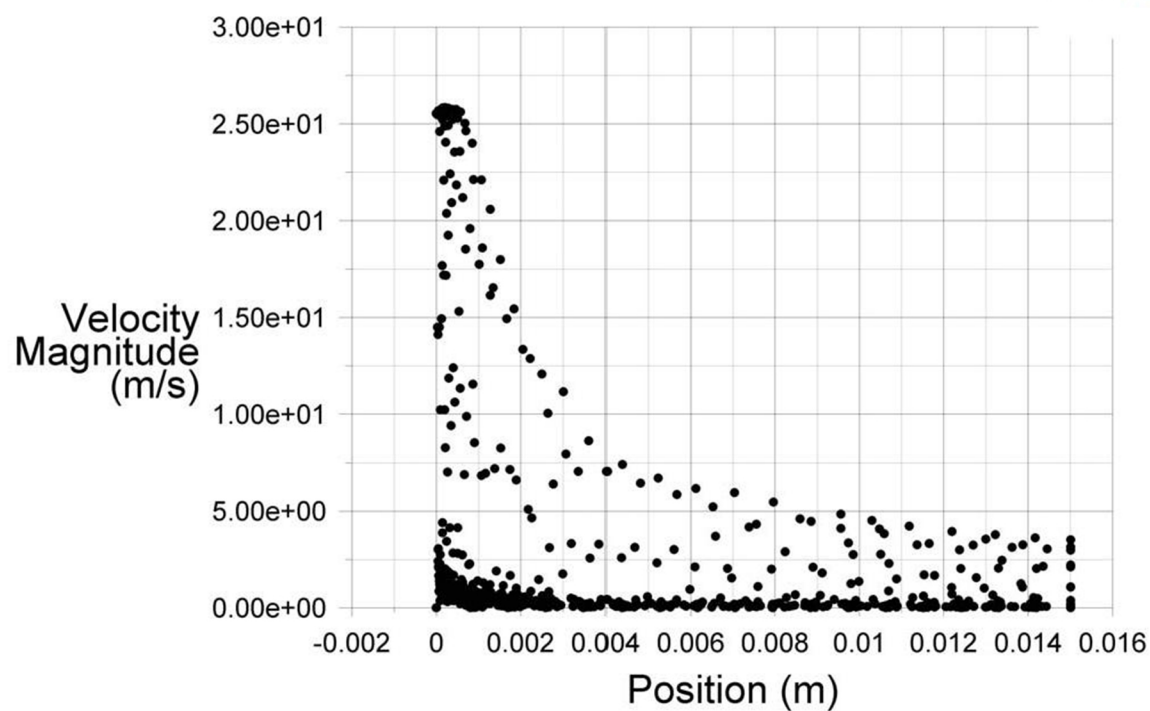


Total Temperature

Jul 18, 2013
ANSYS FLUENT 14.0 (3d, pbns, rke)

• symmetry

ANSYS
14.0



Velocity Magnitude

Jul 18, 2013
ANSYS FLUENT 14.0 (3d, pbns, rke)

0.5 MM DIAMETER

Constants

Sat temperature	194.5 K
Boiling temp	194.5 K
Triple point temp	216.4 K
Surface tension	0.02186 kg/s ²
Density of air	1.225 kg/m ³
Density of vapor CO ₂	1.7878 kg/m ³
Density of liq CO ₂	1032 kg/m ³
Density of solid CO ₂	1562 kg/m ³
Critical weber no.	18
Molar weight	44.01 g/mol
Gas constant	8.314 m ³ Pa/K-mol
Latent heat of vap	571.08 kJ/kg
Latent heat of fusion	196.104 kJ/kg
Cp,v	0.8390 kJ/kg-K
Cp,l	2.0458 kJ/kg-K
Cp,s	1.1580 kJ/kg-K

Aerodynamic break-up (isothermal)

Initial velocity, u	25.5 m/s	
Distance	0.00040 m	
Time	1.569E-05 s	
Droplet velocity	6.243E-06 m/s	Eq. 1
Average diameter	1.132E-04 m	Eq. 2

Thermodynamic break-up

Iteration 1:

CHECK FOR TEMPERATURE

T _{min}	195.34 K	Eq. 5
T _{bulk}	288 K	

NUCLEATION AND BUBBLE GROWTH

Vapor pressure	45 bar	
Flux, Q	296165 g/m ² s	Eq. 4
Radius growth rate	1.916 m/s	Eq. 3
Diameter growth	3.831 m/s	

BLASTING

Starting point	0.00040 m from (0,0)
Initial diameter	1.132E-04 m
Target diameter	2.263E-04 m
Difference	1.132E-04 m
Time taken	2.9533E-05 s
Jet velocity	25.75 m/s
Distance travelled	7.605E-04 m
Current distance	0.00116 m from (0,0)

Random number	4.946
Diameter of droplet	4.5755E-05 m

Iteration 2:

CHECK FOR TEMPERATURE

T _{min}	196.57 K	Eq. 5
T _{bulk}	266 K	

NUCLEATION AND BUBBLE GROWTH

Vapor pressure	29 bar	
Flux, Q	190862 g/m ² s	Eq. 4
Radius growth rate	1.655 m/s	Eq. 3
Diameter growth	3.309 m/s	

BLASTING

Starting point	0.00116 m from (0,0)
Initial diameter	4.5755E-05 m
Target diameter	9.1509E-05 m
Difference	4.5755E-05 m
Time taken	1.3826E-05 s
Jet velocity	21 m/s
Distance travelled	2.903E-04 m
Current distance	0.00145 m from (0,0)

Random number	4.946
Diameter of droplet	1.8502E-05 m

Iteration 3:

CHECK FOR TEMPERATURE

T _{min}	199.61 K	Eq. 5
T _{bulk}	257 K	

NUCLEATION AND BUBBLE GROWTH

Vapor pressure	23 bar	Eq. 4
Flux, Q	151373 g/m ² s	
Radius growth rate	1.532 m/s	Eq. 3
Diameter growth	3.063 m/s	

BLASTING

Starting point	0.00145 m from (0,0)
Initial diameter	1.8502E-05 m
Target diameter	3.7003E-05 m
Difference	1.8502E-05 m
Time taken	6.0399E-06 s
Jet velocity	17.75 m/s
Distance travelled	1.072E-04 m
Current distance	0.00156 m from (0,0)

Random number	4.946
Diameter of droplet	7.4815E-06 m

Iteration 4:

CHECK FOR TEMPERATURE

T _{min}	207.15 K	Eq. 5
T _{bulk}	254 K	

NUCLEATION AND BUBBLE GROWTH

Vapor pressure	20 bar	Eq. 4
Flux, Q	131629 g/m ² s	
Radius growth rate	1.462 m/s	Eq. 3
Diameter growth	2.924 m/s	

BLASTING

Starting point	0.00156 m from (0,0)
Initial diameter	7.4815E-06 m
Target diameter	1.496E-05 m
Difference	7.4815E-06 m
Time taken	2.5588E-06 s
Jet velocity	17 m/s
Distance travelled	4.35E-05 m
Current distance	0.00160 m from (0,0)

Random number	4.946
Diameter of droplet	3.0253E-06 m

Iteration 5:

CHECK FOR TEMPERATURE

T _{min}	225.78 K	Eq. 5
T _{bulk}	250 K	

NUCLEATION AND BUBBLE GROWTH

Vapor pressure	17 bar	Eq. 4
Flux, Q	111884 g/m ² s	
Radius growth rate	1.385 m/s	Eq. 3
Diameter growth	2.770 m/s	

BLASTING

Starting point	0.00160 m from (0,0)
Initial diameter	3.0253E-06 m
Target diameter	6.0505E-06 m
Difference	3.0253E-06 m
Time taken	1.0923E-06 s
Jet velocity	16.5 m/s
Distance travelled	1.8023E-05 m
Current distance	0.00162 m from (0,0)

Random number	4.946
Diameter of droplet	1.2233E-06 m

Iteration 6:

CHECK FOR TEMPERATURE

T _{min}	271.85 K	Eq. 5
T _{bulk}	249 K	

Evaporation and Solidification

Final diameter	1.048E-06 m	Eq. 6
Experimental	1.000E-06 m	
Deviation	-4.800542 %	

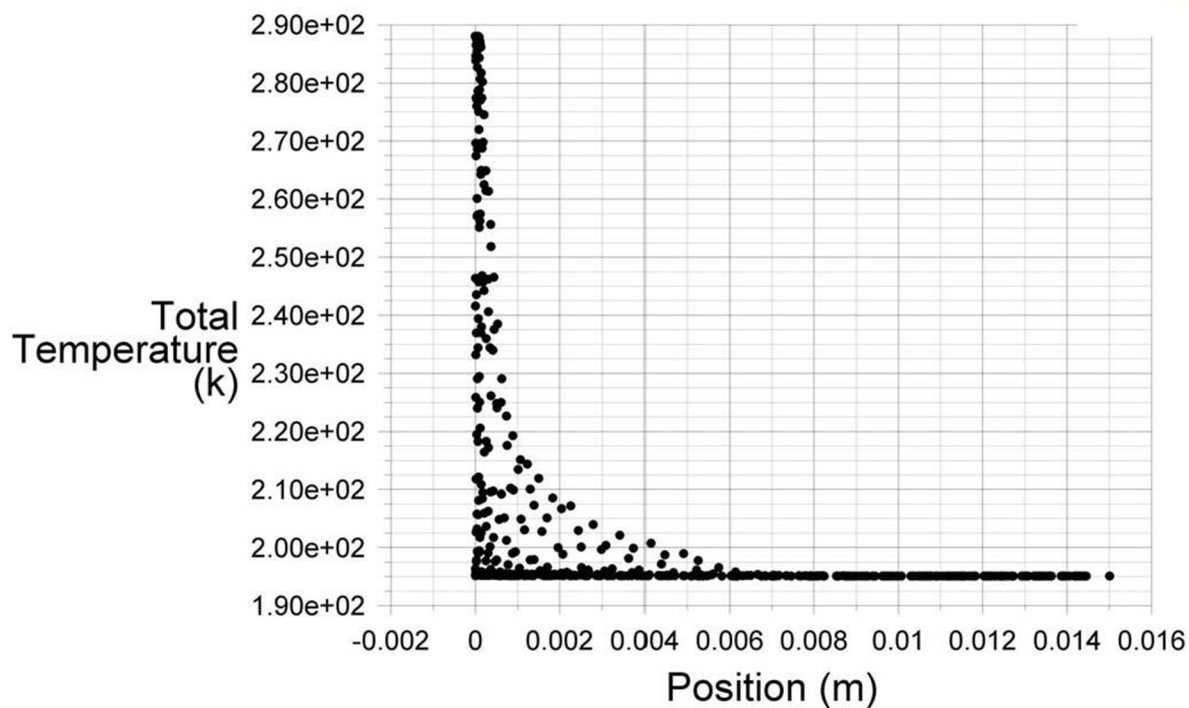
APPENDIX III

CFD SIMULATION AND MATHEMATICAL CALCULATION OF CO₂ EXPANSION THROUGH 0.1 MM, 0.15 MM, 0.2 MM, 0.3 MM, AND 0.4 MM DIAMETER NOZZLE

0.1 MM DIAMETER

• symmetry

ANSYS
14.0

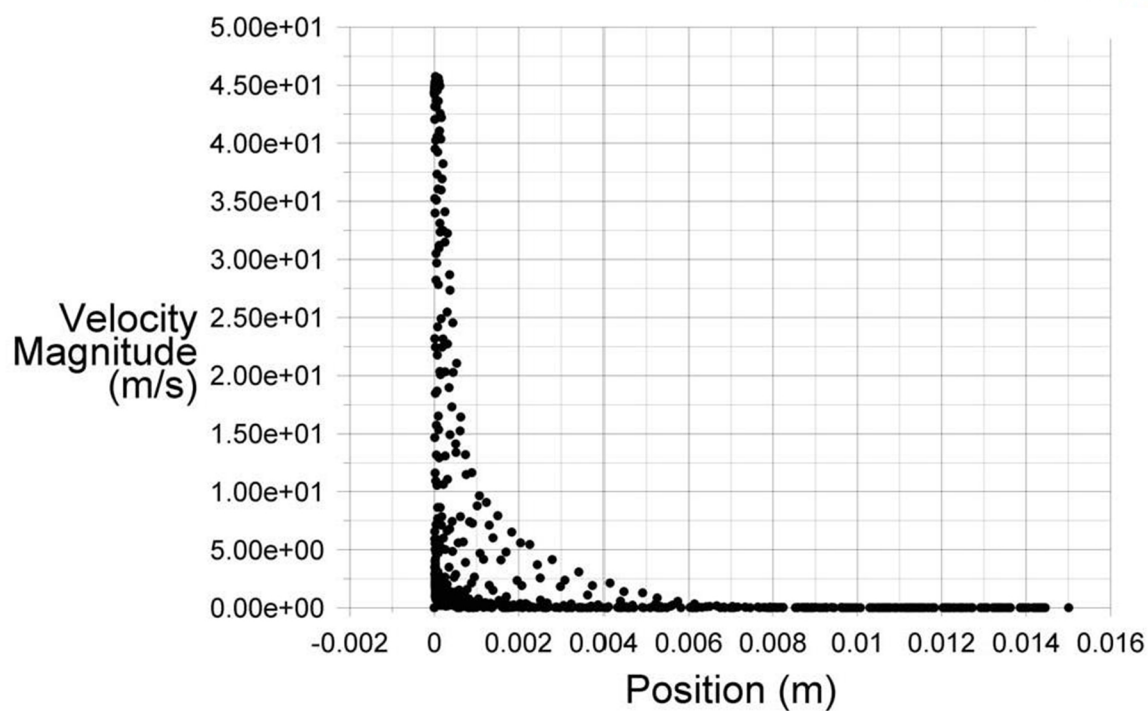


Total Temperature

Jul 18, 2013
ANSYS FLUENT 14.0 (3d, pbns, rke)

• symmetry

ANSYS
14.0



Velocity Magnitude

Jul 18, 2013
ANSYS FLUENT 14.0 (3d, pbns, rke)

0.1 MM DIAMETER

Constants

Sat temperature	194.5 K
Boiling temp	194.5 K
Triple point temp	216.4 K
Surface tension	21.86 dyn/cm
Density of air	1.225 kg/m ³
Density of vapor CO ₂	1.7878 kg/m ³
Density of liq CO ₂	1032 kg/m ³
Density of solid CO ₂	1562 kg/m ³
Critical weber no.	18
Molar weight	44.01 g/mol
Gas constant	8.314 m ³ Pa/K-mol
Latent heat of vap	571.08 kJ/kg
Latent heat of fusion	196.104 kJ/kg
C _{p,v}	0.8390 kJ/kg-K
C _{p,l}	2.0458 kJ/kg-K
C _{p,s}	1.1580 kJ/kg-K

Aerodynamic break-up (isothermal)

Initial velocity, u	46.5 m/s
Distance	0.00010 m
Time	2.151E-06 s
Droplet velocity	1.561E-06 m/s
Average diameter	3.597E-05 m

Thermodynamic break-up

Iteration 1:

CHECK FOR TEMPERATURE

T _{min}	197.13 K
T _{bulk}	288 K

NUCLEATION AND BUBBLE GROWTH

Vapor pressure	45 bar
Flux, Q	296165 g/m ² s
Radius growth rate	1.916 m/s
Diameter growth	3.831 m/s

BLASTING

Starting point	0.00010 m from (0,0)
Initial diameter	3.597E-05 m
Target diameter	7.195E-05 m
Difference	3.597E-05 m
Time taken	9.389E-06 s
Jet velocity	43 m/s
Distance travelled	4.037E-04 m
Current distance	0.00050 m from (0,0)

Random number	4.946
Diameter of droplet	1.455E-05 m

Iteration 2:

CHECK FOR TEMPERATURE

T _{min}	201.00 K
T _{bulk}	240 K

NUCLEATION AND BUBBLE GROWTH

Vapor pressure	16 bar
Flux, Q	105303 g/m ² s
Radius growth rate	1.357 m/s
Diameter growth	2.714 m/s

BLASTING

Starting point	0.00050 m from (0,0)
Initial diameter	1.455E-05 m
Target diameter	2.909E-05 m
Difference	1.455E-05 m
Time taken	5.359E-06 s
Jet velocity	22.5 m/s
Distance travelled	1.206E-04 m
Current distance	0.00062 m from (0,0)

Random number	4.946
Diameter of droplet	5.882E-06 m

Iteration 3:

CHECK FOR TEMPERATURE

Tmin	210.59 K
Tbulk	233 K

NUCLEATION AND BUBBLE GROWTH

Vapor pressure	10 bar
Flux, Q	65814 g/m ² s
Radius growth rate	1.160 m/s
Diameter growth	2.321 m/s

BLASTING

Starting point	0.00062 m from (0,0)
Initial diameter	5.882E-06 m
Target diameter	1.176E-05 m
Difference	5.882E-06 m
Time taken	2.535E-06 s
Jet velocity	17 m/s
Distance travelled	4.309E-05 m
Current distance	0.00067 m from (0,0)

Random number	4.946
Diameter of droplet	2.644E-06 m

Iteration 4:

CHECK FOR TEMPERATURE

Tmin	230.29 K
Tbulk	231 K

NUCLEATION AND BUBBLE GROWTH

Vapor pressure	9 bar
Flux, Q	59233 g/m ² s
Radius growth rate	1.120 m/s
Diameter growth	2.241 m/s

BLASTING

Starting point	0.00067 m from (0,0)
Initial diameter	2.644E-06 m
Target diameter	5.287E-06 m
Difference	2.644E-06 m
Time taken	1.180E-06 s
Jet velocity	16.5 m/s
Distance travelled	1.947E-05 m
Current distance	0.00069 m from (0,0)

Random number	4.946
Diameter of droplet	1.069E-06 m

Iteration 4:

CHECK FOR TEMPERATURE

Tmin	283.02 K
Tbulk	229 K

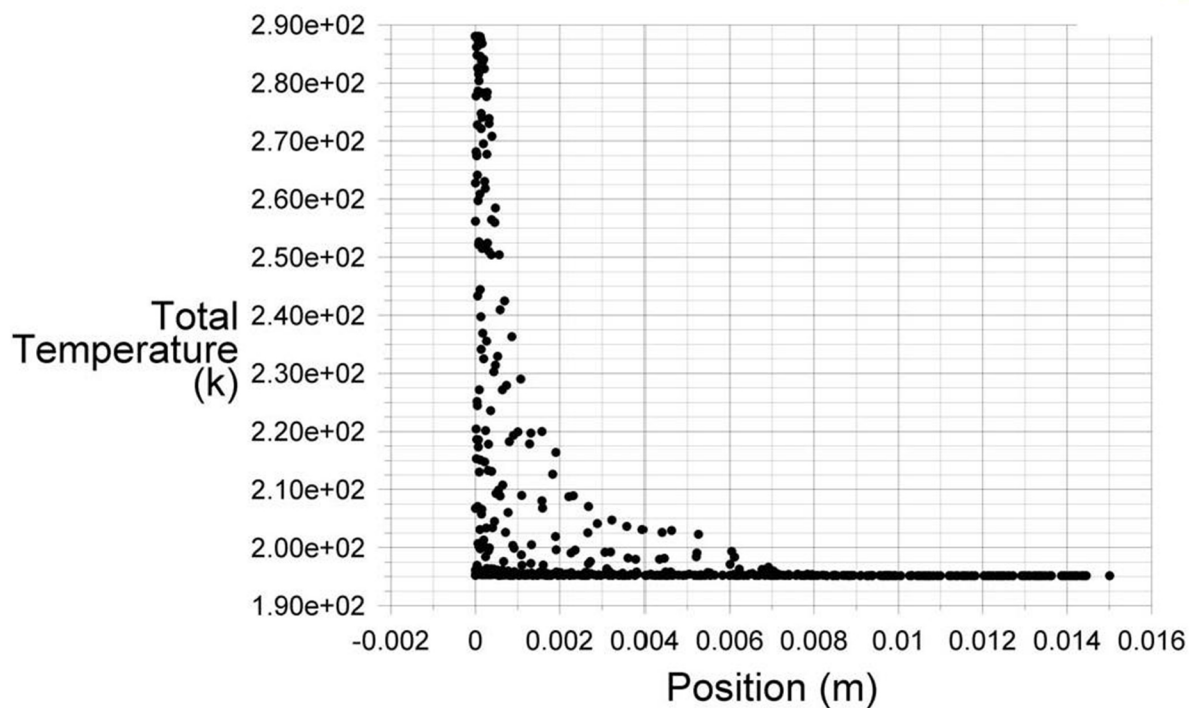
Evaporation and Solidification

Final diameter	8.906E-07 m
Experimental	9.00E-07 m
Deviation	1.043405 %

0.15 MM DIAMETER

• symmetry

ANSYS
14.0

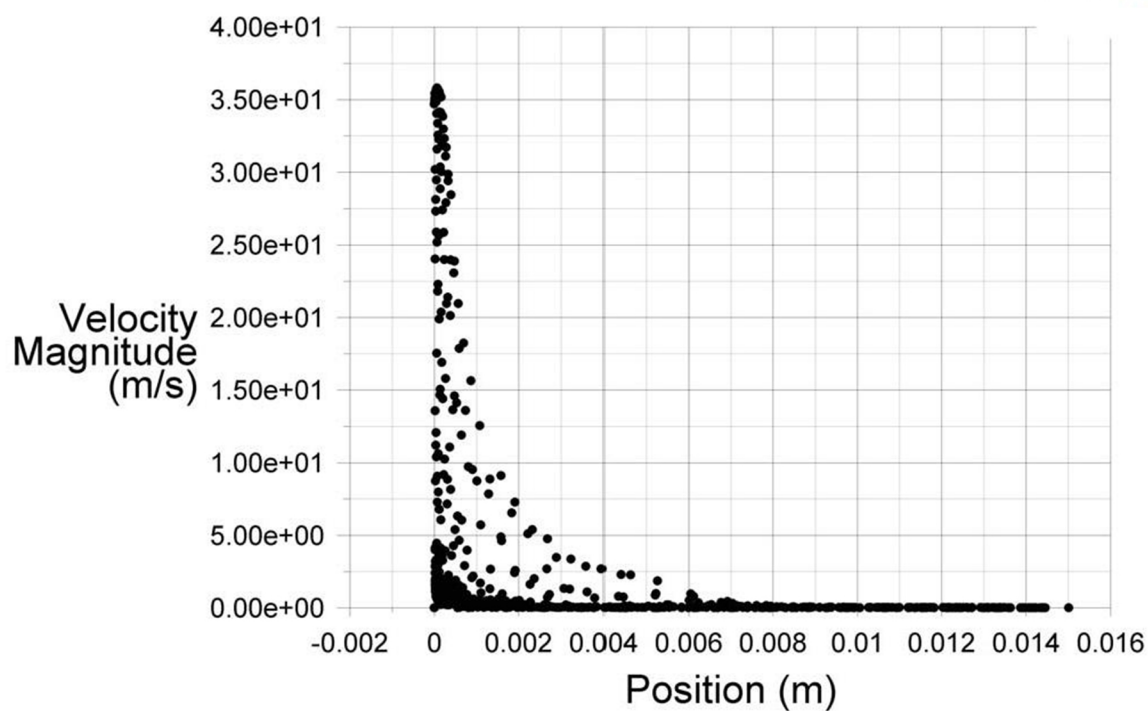


Total Temperature

Jul 29, 2013
ANSYS FLUENT 14.0 (3d, pbns, rke)

• symmetry

ANSYS
14.0



Velocity Magnitude

Jul 29, 2013
ANSYS FLUENT 14.0 (3d, pbns, rke)

0.15 MM DIAMETER

Constants

Sat temperature	194.5 K
Boiling temp	194.5 K
Triple point temp	216.4 K
Surface tension	21.86 dyn/cm
Density of air	1.225 kg/m ³
Density of vapor CO ₂	1.7878 kg/m ³
Density of liq CO ₂	1032 kg/m ³
Density of solid CO ₂	1562 kg/m ³
Critical weber no.	18
Molar weight	44.01 g/mol
Gas constant	8.314 m ³ Pa/K-mol
Latent heat of vap	571.08 kJ/kg
Latent heat of fusion	196.104 kJ/kg
C _{p,v}	0.8390 kJ/kg-K
C _{p,l}	2.0458 kJ/kg-K
C _{p,s}	1.1580 kJ/kg-K

Aerodynamic break-up (isothermal)

Initial velocity, u	36 m/s
Distance	0.00015 m
Time	4.167E-06 s
Droplet velocity	2.341E-06 m/s
Average diameter	5.677E-05 m

Thermodynamic break-up

Iteration 1:

CHECK FOR TEMPERATURE

T _{min}	196.17 K
T _{bulk}	288 K

NUCLEATION AND BUBBLE GROWTH

Vapor pressure	45 bar
Flux, Q	296165 g/m ² s
Radius growth rate	1.916 m/s
Diameter growth	3.831 m/s

BLASTING

Starting point	0.00015 m from (0,0)
Initial diameter	5.677E-05 m
Target diameter	1.135E-04 m
Difference	5.677E-05 m
Time taken	1.482E-05 s
Jet velocity	35 m/s
Distance travelled	5.186E-04 m
Current distance	0.00067 m from (0,0)

Random number	4.946
Diameter of droplet	2.103E-05 m

Iteration 2:

CHECK FOR TEMPERATURE

T _{min}	199.00 K
T _{bulk}	245 K

NUCLEATION AND BUBBLE GROWTH

Vapor pressure	15 bar
Flux, Q	98722 g/m ² s
Radius growth rate	1.328 m/s
Diameter growth	2.656 m/s

BLASTING

Starting point	0.00067 m from (0,0)
Initial diameter	2.103E-05 m
Target diameter	4.205E-05 m
Difference	2.103E-05 m
Time taken	7.915E-06 s
Jet velocity	18 m/s
Distance travelled	1.425E-04 m
Current distance	0.00081 m from (0,0)

Random number	4.946
---------------	-------

Iteration 3:

CHECK FOR TEMPERATURE

Tmin	206.65 K
Tbulk	238 K

NUCLEATION AND BUBBLE GROWTH

Vapor pressure	13 bar
Flux, Q	85559 g/m ² s
Radius growth rate	1.266 m/s
Diameter growth	2.533 m/s

Iteration 4:

CHECK FOR TEMPERATURE

Tmin	227.31 K
Tbulk	236 K

NUCLEATION AND BUBBLE GROWTH

Vapor pressure	12 bar
Flux, Q	78977 g/m ² s
Radius growth rate	1.233 m/s
Diameter growth	2.466 m/s

Iteration 4:

CHECK FOR TEMPERATURE

Tmin	281.44 K
Tbulk	235 K

Evaporation and Solidification

Final diameter	9.146E-07 m
----------------	-------------

Diameter of droplet	7.788E-06 m
---------------------	-------------

BLASTING

Starting point	0.00081 m from (0,0)
Initial diameter	7.788E-06 m
Target diameter	1.558E-05 m
Difference	7.788E-06 m
Time taken	3.075E-06 s
Jet velocity	16 m/s
Distance travelled	4.920E-05 m
Current distance	0.00086 m from (0,0)

Random number	4.946
Diameter of droplet	2.884E-06 m

BLASTING

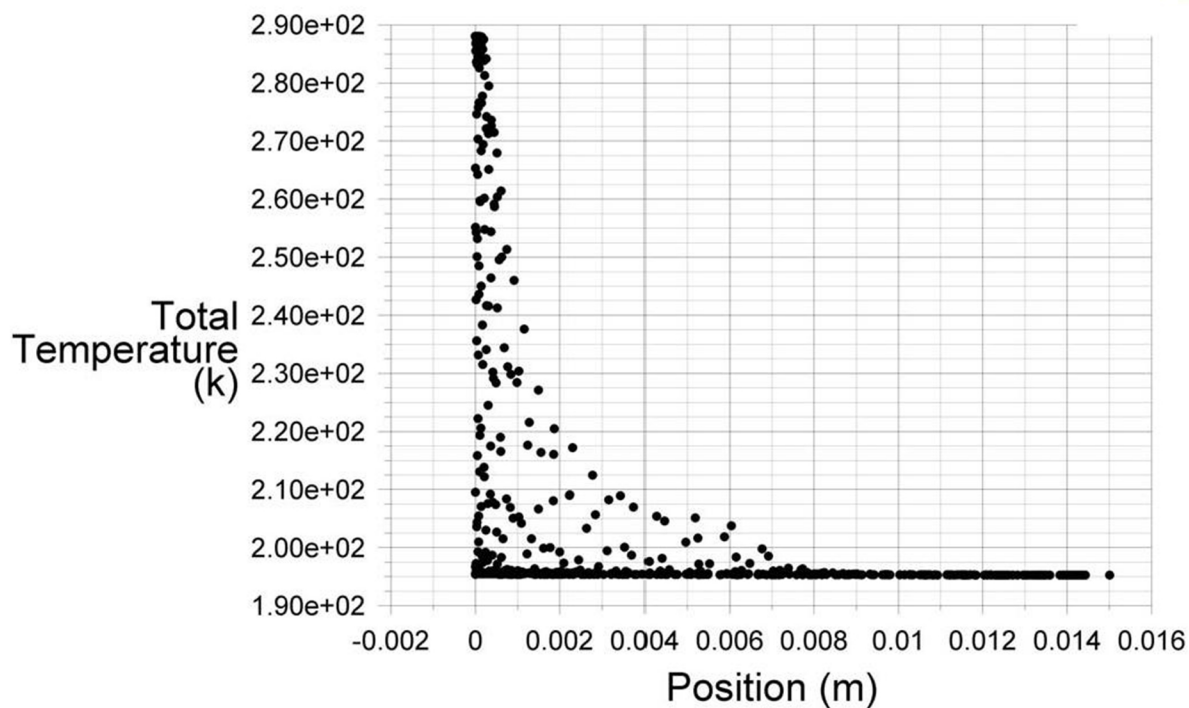
Starting point	0.00086 m from (0,0)
Initial diameter	2.884E-06 m
Target diameter	5.769E-06 m
Difference	2.884E-06 m
Time taken	1.170E-06 s
Jet velocity	15 m/s
Distance travelled	1.754E-05 m
Current distance	0.00088 m from (0,0)

Random number	4.946
Diameter of droplet	1.088E-06 m

0.2 MM DIAMETER

• symmetry

ANSYS
14.0

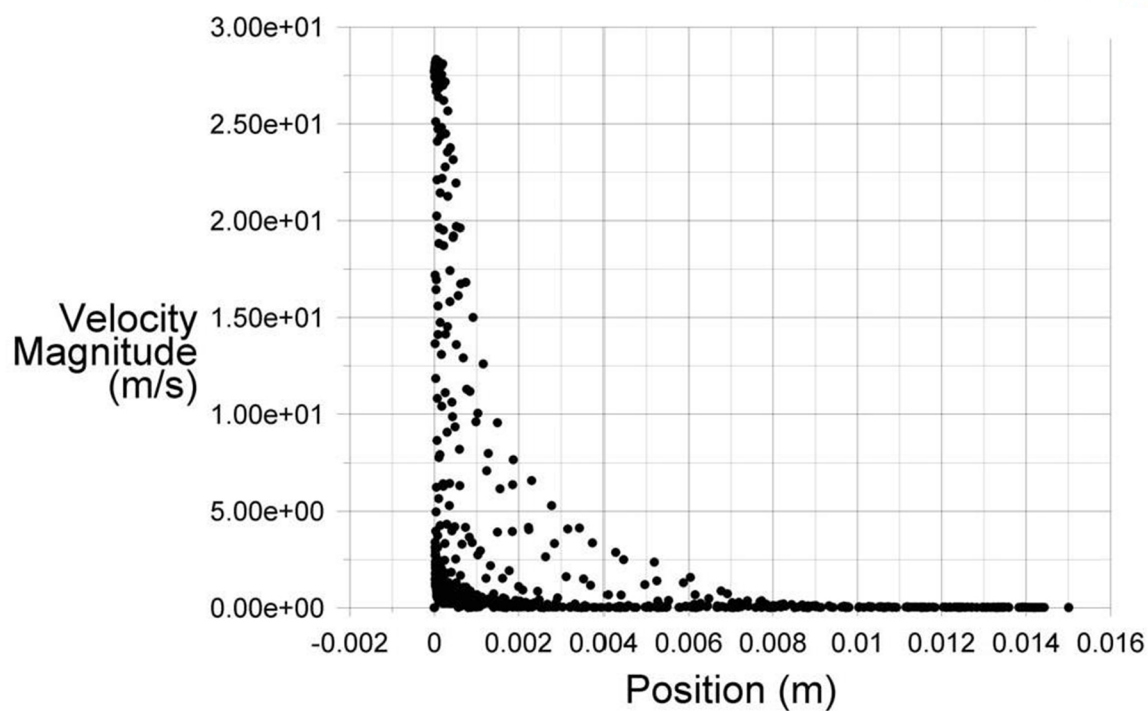


Total Temperature

Jul 18, 2013
ANSYS FLUENT 14.0 (3d, pbns, rke)

• symmetry

ANSYS
14.0



Velocity Magnitude

Jul 18, 2013
ANSYS FLUENT 14.0 (3d, pbns, rke)

0.2 MM DIAMETER

Constants

Sat temperature	194.5 K
Boiling temp	194.5 K
Triple point temp	216.4 K
Surface tension	21.86 dyn/cm
Density of air	1.225 kg/m ³
Density of vapor CO ₂	1.7878 kg/m ³
Density of liq CO ₂	1032 kg/m ³
Density of solid CO ₂	1562 kg/m ³
Critical weber no.	18
Molar weight	44.01 g/mol
Gas constant	8.314 m ³ Pa/K-mol
Latent heat of vap	571.08 kJ/kg
Latent heat of fusion	196.104 kJ/kg
C _{p,v}	0.8390 kJ/kg-K
C _{p,l}	2.0458 kJ/kg-K
C _{p,s}	1.1580 kJ/kg-K

Aerodynamic break-up (isothermal)

Initial velocity, u	28.5 m/s
Distance	0.00020 m
Time	7.018E-06 s
Droplet velocity	3.122E-06 m/s
Average diameter	9.321E-05 m

Thermodynamic break-up

Iteration 1:

CHECK FOR TEMPERATURE

T _{min}	195.52 K
T _{bulk}	288 K

NUCLEATION AND BUBBLE GROWTH

Vapor pressure	45 bar
Flux, Q	296165 g/m ² s
Radius growth rate	1.916 m/s
Diameter growth	3.831 m/s

BLASTING

Starting point	0.00020 m from (0,0)
Initial diameter	9.321E-05 m
Target diameter	1.864E-04 m
Difference	9.321E-05 m
Time taken	2.4329E-05 s
Jet velocity	28 m/s
Distance travelled	6.812E-04 m
Current distance	0.00088 m from (0,0)

Random number	4.946
Diameter of droplet	3.7691E-05 m

Iteration 2:

CHECK FOR TEMPERATURE

T _{min}	197.01 K
T _{bulk}	245 K

NUCLEATION AND BUBBLE GROWTH

Vapor pressure	15 bar
Flux, Q	98722 g/m ² s
Radius growth rate	1.328 m/s
Diameter growth	2.656 m/s

BLASTING

Starting point	0.00088 m from (0,0)
Initial diameter	3.7691E-05 m
Target diameter	7.5382E-05 m
Difference	3.7691E-05 m
Time taken	1.4188E-05 s
Jet velocity	15 m/s
Distance travelled	2.128E-04 m
Current distance	0.00109 m from (0,0)

Random number	4.946
---------------	-------

Iteration 3:

CHECK FOR TEMPERATURE

Tmin	200.71 K
Tbulk	238 K

NUCLEATION AND BUBBLE GROWTH

Vapor pressure	12.5 bar
Flux, Q	82268 g/m ² s
Radius growth rate	1.250 m/s
Diameter growth	2.500 m/s

Iteration 4:

CHECK FOR TEMPERATURE

Tmin	208.78 K
Tbulk	234 K

NUCLEATION AND BUBBLE GROWTH

Vapor pressure	11 bar
Flux, Q	72396 g/m ² s
Radius growth rate	1.198 m/s
Diameter growth	2.396 m/s

Iteration 5:

CHECK FOR TEMPERATURE

Tmin	228.77 K
Tbulk	233 K

NUCLEATION AND BUBBLE GROWTH

Vapor pressure	11 bar
Flux, Q	72396 g/m ² s
Radius growth rate	1.198 m/s
Diameter growth	2.396 m/s

Iteration 6:

CHECK FOR TEMPERATURE

Tmin	279.25 K
Tbulk	233 K

Evaporation and Solidification

Final diameter	9.3554E-07 m
Literature deviation	9.50E-07 m 1.52 %

Diameter of droplet	1.5241E-05 m
---------------------	--------------

BLASTING

Starting point	0.00109 m from (0,0)
Initial diameter	1.5241E-05 m
Target diameter	3.048E-05 m
Difference	1.5241E-05 m
Time taken	6.097E-06 s
Jet velocity	12.5 m/s
Distance travelled	7.621E-05 m
Current distance	0.00117 m from (0,0)

Random number	4.946
Diameter of droplet	6.627E-06 m

BLASTING

Starting point	0.00117 m from (0,0)
Initial diameter	6.6265E-06 m
Target diameter	1.325E-05 m
Difference	6.6265E-06 m
Time taken	2.7662E-06 s
Jet velocity	11 m/s
Distance travelled	3.0428E-05 m
Current distance	0.00120 m from (0,0)

Random number	4.946
Diameter of droplet	2.761E-06 m

BLASTING

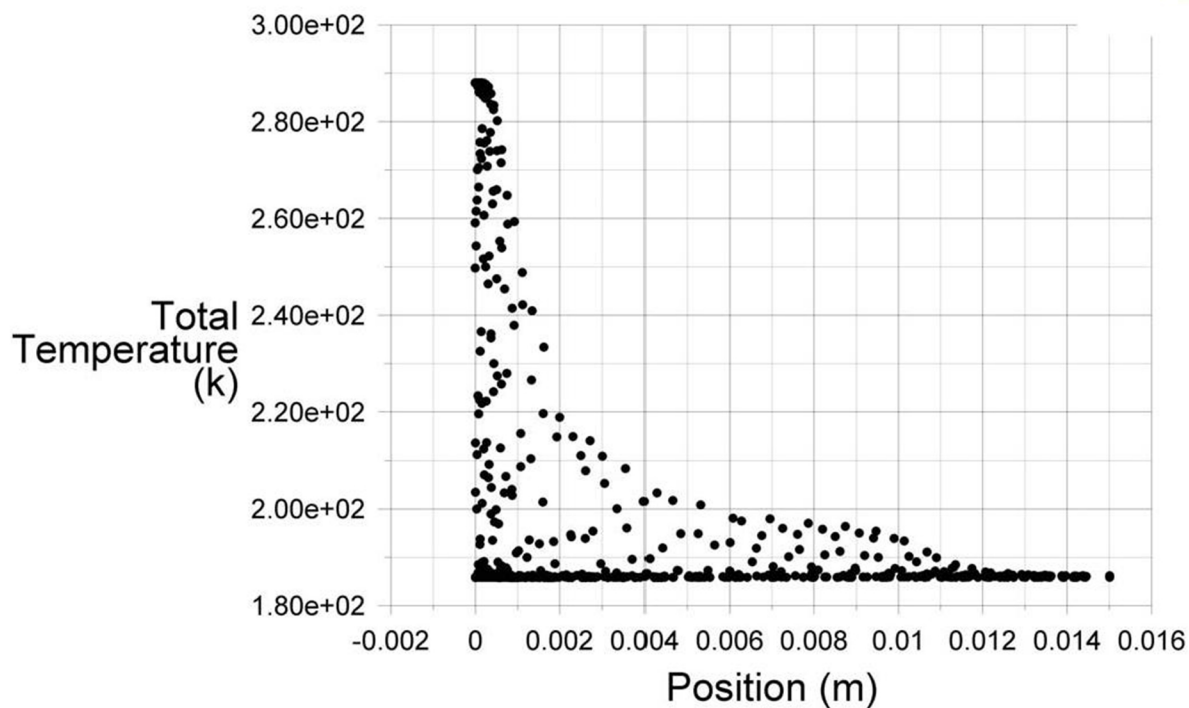
Starting point	0.00120 m from (0,0)
Initial diameter	2.761E-06 m
Target diameter	5.522E-06 m
Difference	2.761E-06 m
Time taken	1.1526E-06 s
Jet velocity	10 m/s
Distance travelled	1.1526E-05 m
Current distance	0.00121 m from (0,0)

Random number	4.946
Diameter of droplet	1.1165E-06 m

0.3 MM DIAMETER

• symmetry

ANSYS
14.0

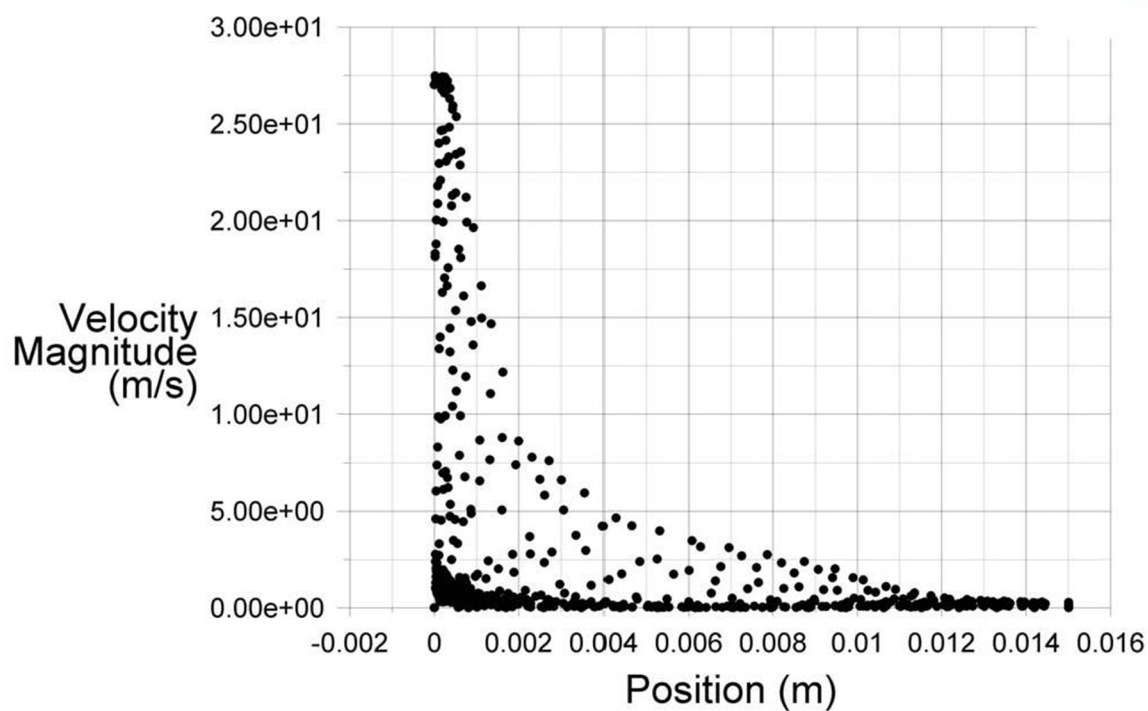


Total Temperature

Jul 27, 2013
ANSYS FLUENT 14.0 (3d, pbns, rke)

• symmetry

ANSYS
14.0



Velocity Magnitude

Jul 27, 2013
ANSYS FLUENT 14.0 (3d, pbns, rke)

0.3 MM DIAMETER

Constants

Sat temperature	194.5 K
Boiling temp	194.5 K
Triple point temp	216.4 K
Surface tension	0.02186 kg/s ²
Density of air	1.225 kg/m ³
Density of vapor CO ₂	1.7878 kg/m ³
Density of liq CO ₂	1032 kg/m ³
Density of solid CO ₂	1562 kg/m ³
Critical weber no.	18
Molar weight	44.01 g/mol
Gas constant	8.314 m ³ Pa/K-mol
Latent heat of vap	571.08 kJ/kg
Latent heat of fusion	196.104 kJ/kg
C _{p,v}	0.8390 kJ/kg-K
C _{p,l}	2.0458 kJ/kg-K
C _{p,s}	1.1580 kJ/kg-K

Aerodynamic break-up (isothermal)

Initial velocity, u	27.5 m/s	
Distance	0.00028 m	
Time	1.000E-05 s	
Droplet velocity	4.292E-06 m/s	Eq. 1
Average diameter	1.001E-04 m	Eq. 2

Thermodynamic break-up

Iteration 1:

CHECK FOR TEMPERATURE

T _{min}	195.45 K	Eq. 5
T _{bulk}	288 K	

NUCLEATION AND BUBBLE GROWTH

Vapor pressure	45 bar	
Flux, Q	296165 g/m ² s	Eq. 4
Radius growth rate	1.916 m/s	Eq. 3
Diameter growth	3.831 m/s	

BLASTING

Starting point	0.00028 m from (0,0)
Initial diameter	1.001E-04 m
Target diameter	2.002E-04 m
Difference	1.001E-04 m
Time taken	2.613E-05 s
Jet velocity	27.25 m/s
Distance travelled	7.120E-04 m
Current distance	0.00099 m from (0,0)

Random number	4.946
Diameter of droplet	4.048E-05 m

Iteration 2:

CHECK FOR TEMPERATURE

T _{min}	196.84 K	Eq. 5
T _{bulk}	252 K	

NUCLEATION AND BUBBLE GROWTH

Vapor pressure	20 bar	
Flux, Q	131629 g/m ² s	Eq. 4
Radius growth rate	1.462 m/s	Eq. 3
Diameter growth	2.924 m/s	

BLASTING

Starting point	0.00099 m from (0,0)
Initial diameter	4.0482E-05 m
Target diameter	8.0964E-05 m
Difference	4.0482E-05 m
Time taken	1.3846E-05 s
Jet velocity	18.2 m/s
Distance travelled	2.520E-04 m
Current distance	0.00124 m from (0,0)

Random number	4.946
Diameter of droplet	1.637E-05 m

Iteration 3:

CHECK FOR TEMPERATURE

T _{min}	200.28 K	Eq. 5
T _{bulk}	242 K	

NUCLEATION AND BUBBLE GROWTH

Vapor pressure	13 bar	Eq. 4
Flux, Q	85559 g/m ² s	
Radius growth rate	1.266 m/s	Eq. 3
Diameter growth	2.533 m/s	

BLASTING

Starting point	0.00124 m from (0,0)
Initial diameter	1.637E-05 m
Target diameter	3.2739E-05 m
Difference	1.637E-05 m
Time taken	6.4632E-06 s
Jet velocity	15.5 m/s
Distance travelled	1.002E-04 m
Current distance	0.00134 m from (0,0)

Random number	4.946
Diameter of droplet	7.1172E-06 m

Iteration 4:

CHECK FOR TEMPERATURE

T _{min}	207.80 K	Eq. 5
T _{bulk}	238 K	

NUCLEATION AND BUBBLE GROWTH

Vapor pressure	12.5 bar	Eq. 4
Flux, Q	82268 g/m ² s	
Radius growth rate	1.250 m/s	Eq. 3
Diameter growth	2.500 m/s	

BLASTING

Starting point	0.00134 m from (0,0)
Initial diameter	7.1172E-06 m
Target diameter	1.423E-05 m
Difference	7.1172E-06 m
Time taken	2.8471E-06 s
Jet velocity	13 m/s
Distance travelled	3.7012E-05 m
Current distance	0.00138 m from (0,0)

Random number	4.946
Diameter of droplet	2.878E-06 m

Iteration 5:

CHECK FOR TEMPERATURE

T _{min}	227.38 K	Eq. 5
T _{bulk}	236 K	

NUCLEATION AND BUBBLE GROWTH

Vapor pressure	12 bar	Eq. 4
Flux, Q	78977 g/m ² s	
Radius growth rate	1.233 m/s	Eq. 3
Diameter growth	2.466 m/s	

BLASTING

Starting point	0.00138 m from (0,0)
Initial diameter	2.878E-06 m
Target diameter	5.7559E-06 m
Difference	2.878E-06 m
Time taken	1.167E-06 s
Jet velocity	12.5 m/s
Distance travelled	1.4588E-05 m
Current distance	0.00139 m from (0,0)

Random number	4.946
Diameter of droplet	1.1638E-06 m

Iteration 6:

CHECK FOR TEMPERATURE

T _{min}	275.81 K	Eq. 5
T _{bulk}	235 K	

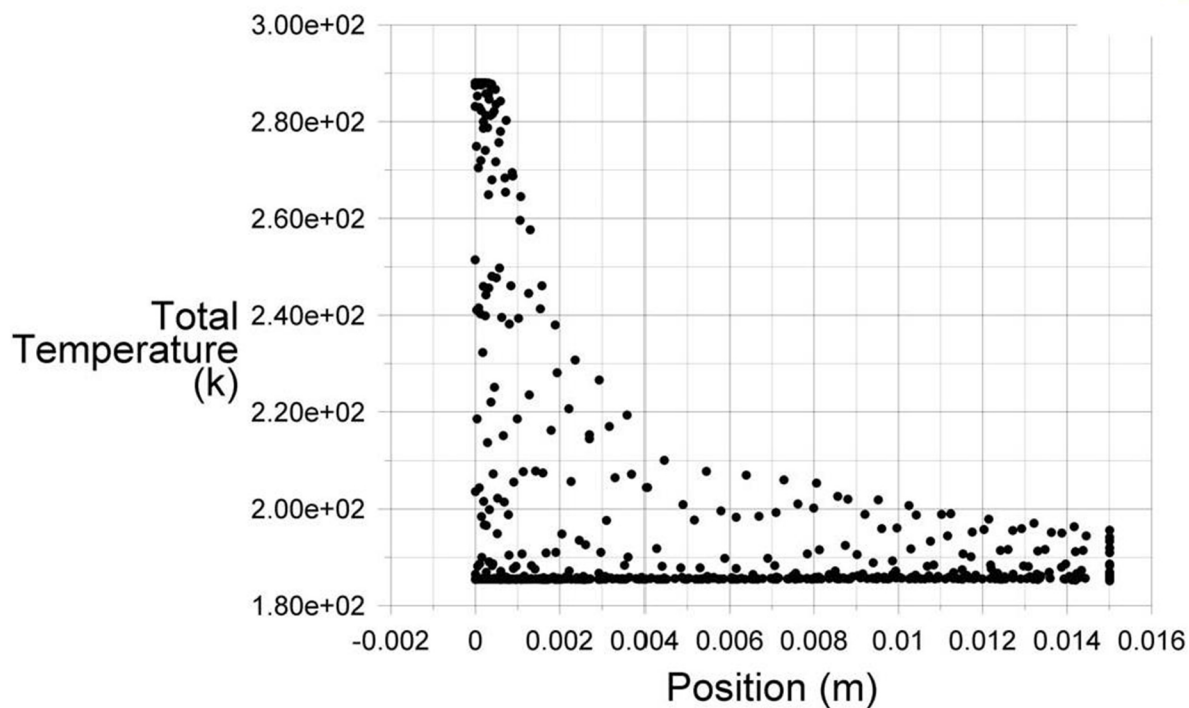
Evaporation and Solidification

Final diameter	9.779E-07 m	Eq. 6
----------------	-------------	-------

0.4 MM DIAMETER

• symmetry

ANSYS
14.0

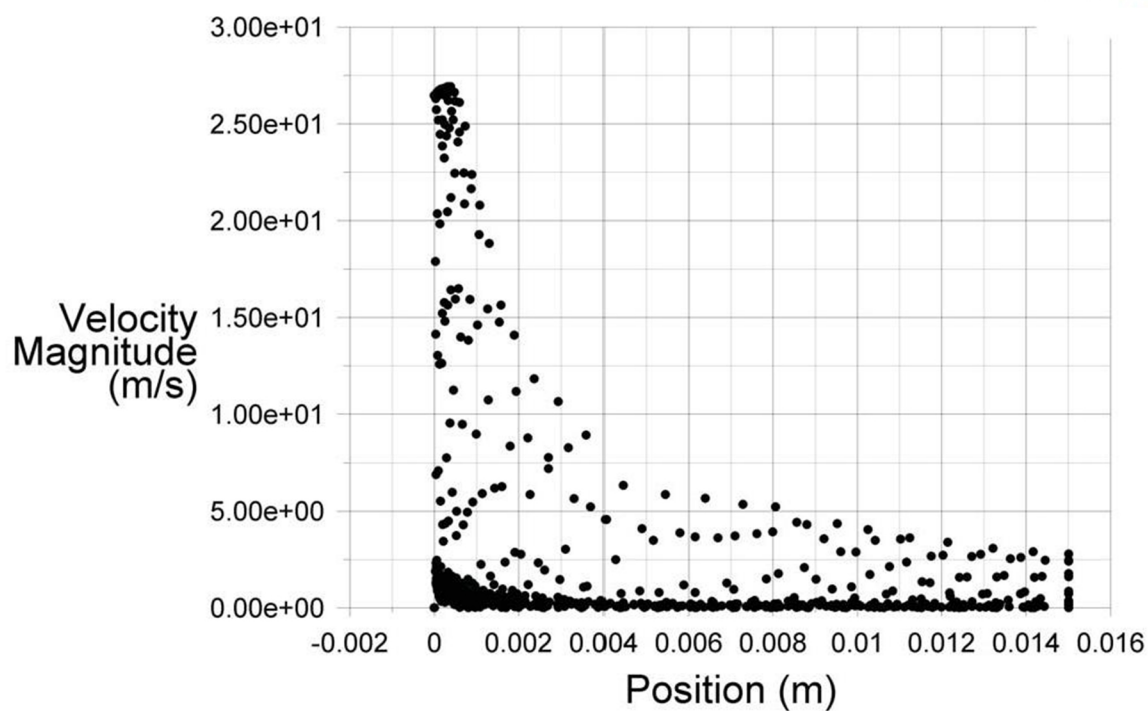


Total Temperature

Jul 26, 2013
ANSYS FLUENT 14.0 (3d, pbns, rke)

• symmetry

ANSYS
14.0



Velocity Magnitude

Jul 26, 2013
ANSYS FLUENT 14.0 (3d, pbns, rke)

0.4 MM DIAMETER

Constants

Sat temperature	194.5 K
Boiling temp	194.5 K
Triple point temp	216.4 K
Surface tension	0.02186 kg/s ²
Density of air	1.225 kg/m ³
Density of vapor CO ₂	1.7878 kg/m ³
Density of liq CO ₂	1032 kg/m ³
Density of solid CO ₂	1562 kg/m ³
Critical weber no.	18
Molar weight	44.01 g/mol
Gas constant	8.314 m ³ Pa/K-mol
Latent heat of vap	571.08 kJ/kg
Latent heat of fusion	196.104 kJ/kg
C _{p,v}	0.8390 kJ/kg-K
C _{p,l}	2.0458 kJ/kg-K
C _{p,s}	1.1580 kJ/kg-K

Aerodynamic break-up (isothermal)

Initial velocity, u	26.5 m/s	
Distance	0.00035 m	
Time	1.321E-05 s	
Droplet velocity	5.463E-06 m/s	Eq. 1
Average diameter	1.108E-04 m	Eq. 2

Thermodynamic break-up

Iteration 1:

CHECK FOR TEMPERATURE

T _{min}	195.35 K	Eq. 5
T _{bulk}	288 K	

NUCLEATION AND BUBBLE GROWTH

Vapor pressure	45 bar	
Flux, Q	296165 g/m ² s	Eq. 4
Radius growth rate	1.916 m/s	Eq. 3
Diameter growth	3.831 m/s	

BLASTING

Starting point	0.00035 m from (0,0)
Initial diameter	1.108E-04 m
Target diameter	2.215E-04 m
Difference	1.108E-04 m
Time taken	2.891E-05 s
Jet velocity	27 m/s
Distance travelled	7.806E-04 m
Current distance	0.00113 m from (0,0)

Random number	4.946
Diameter of droplet	4.479E-05 m

Iteration 2:

CHECK FOR TEMPERATURE

T _{min}	196.61 K	Eq. 5
T _{bulk}	258 K	

NUCLEATION AND BUBBLE GROWTH

Vapor pressure	23 bar	
Flux, Q	151373 g/m ² s	Eq. 4
Radius growth rate	1.532 m/s	Eq. 3
Diameter growth	3.063 m/s	

BLASTING

Starting point	0.00113 m from (0,0)
Initial diameter	4.4789E-05 m
Target diameter	8.9579E-05 m
Difference	4.4789E-05 m
Time taken	1.4622E-05 s
Jet velocity	19 m/s
Distance travelled	2.778E-04 m
Current distance	0.00141 m from (0,0)

Random number	4.946
Diameter of droplet	1.8111E-05 m

Iteration 3:

CHECK FOR TEMPERATURE

T _{min}	199.72 K	Eq. 5
T _{bulk}	250 K	

NUCLEATION AND BUBBLE GROWTH

Vapor pressure	16 bar	Eq. 4
Flux, Q	105303 g/m ² s	Eq. 3
Radius growth rate	1.357 m/s	
Diameter growth	2.714 m/s	

BLASTING

Starting point	0.00141 m from (0,0)
Initial diameter	1.8111E-05 m
Target diameter	3.6223E-05 m
Difference	1.8111E-05 m
Time taken	6.6727E-06 s
Jet velocity	17.5 m/s
Distance travelled	1.168E-04 m
Current distance	0.00153 m from (0,0)

Random number	4.946
Diameter of droplet	7.3236E-06 m

Iteration 4:

CHECK FOR TEMPERATURE

T _{min}	207.42 K	Eq. 5
T _{bulk}	246 K	

NUCLEATION AND BUBBLE GROWTH

Vapor pressure	15 bar	Eq. 4
Flux, Q	98722 g/m ² s	Eq. 3
Radius growth rate	1.328 m/s	
Diameter growth	2.656 m/s	

BLASTING

Starting point	0.00153 m from (0,0)
Initial diameter	7.3236E-06 m
Target diameter	1.465E-05 m
Difference	7.3236E-06 m
Time taken	2.7569E-06 s
Jet velocity	16 m/s
Distance travelled	4.4111E-05 m
Current distance	0.00157 m from (0,0)

Random number	4.946
Diameter of droplet	2.961E-06 m

Iteration 5:

CHECK FOR TEMPERATURE

T _{min}	226.45 K	Eq. 5
T _{bulk}	243 K	

NUCLEATION AND BUBBLE GROWTH

Vapor pressure	14 bar	Eq. 4
Flux, Q	92140 g/m ² s	Eq. 3
Radius growth rate	1.298 m/s	
Diameter growth	2.596 m/s	

BLASTING

Starting point	0.00157 m from (0,0)
Initial diameter	2.9614E-06 m
Target diameter	5.9229E-06 m
Difference	2.9614E-06 m
Time taken	1.1407E-06 s
Jet velocity	15.5 m/s
Distance travelled	1.7681E-05 m
Current distance	0.00159 m from (0,0)

Random number	4.946
Diameter of droplet	1.1975E-06 m

Iteration 6:

CHECK FOR TEMPERATURE

T _{min}	273.52 K	Eq. 5
T _{bulk}	243 K	

Evaporation and Solidification

Final diameter	1.018E-06 m	Eq. 6
----------------	-------------	-------

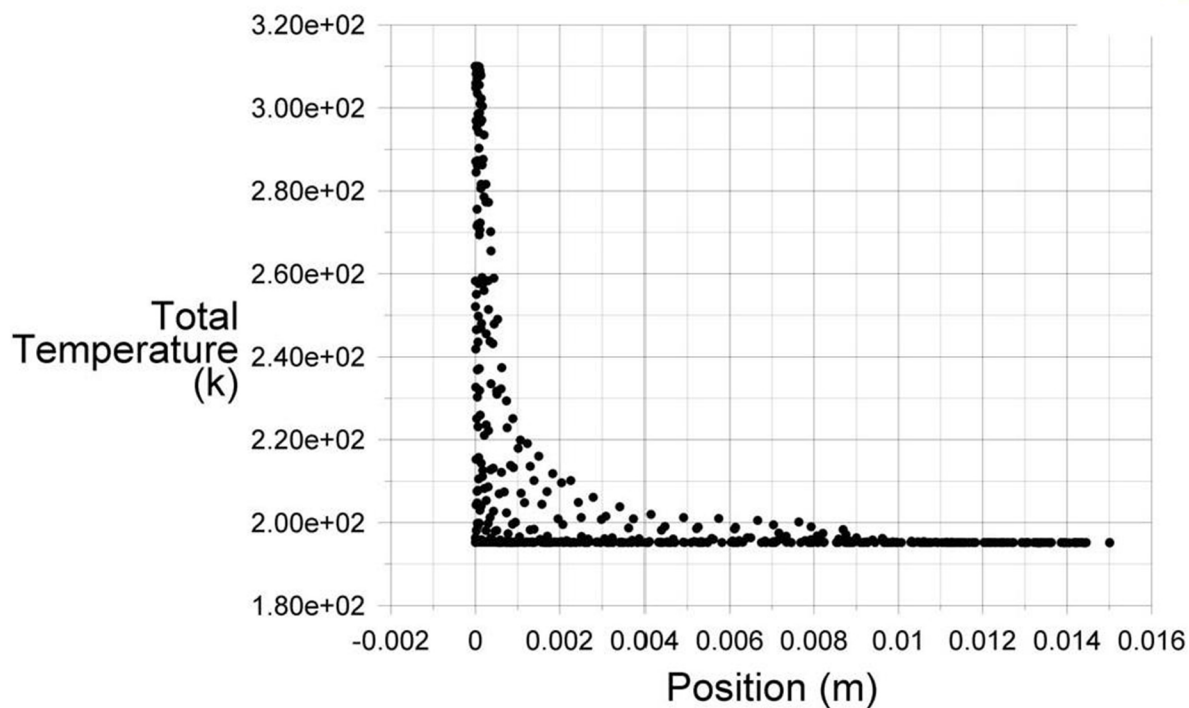
APPENDIX IV

CFD SIMULATION AND MATHEMATICAL CALCULATION OF CO₂ EXPANSION THROUGH 0.1 MM, 0.2 MM, 0.5 MM, 1 MM, AND 2 MM DIAMETER NOZZLE AT SUPERCRITICAL STORAGE CONDITIONS

0.1 MM DIAMETER (SUPERCRITICAL)

• symmetry

ANSYS
14.0

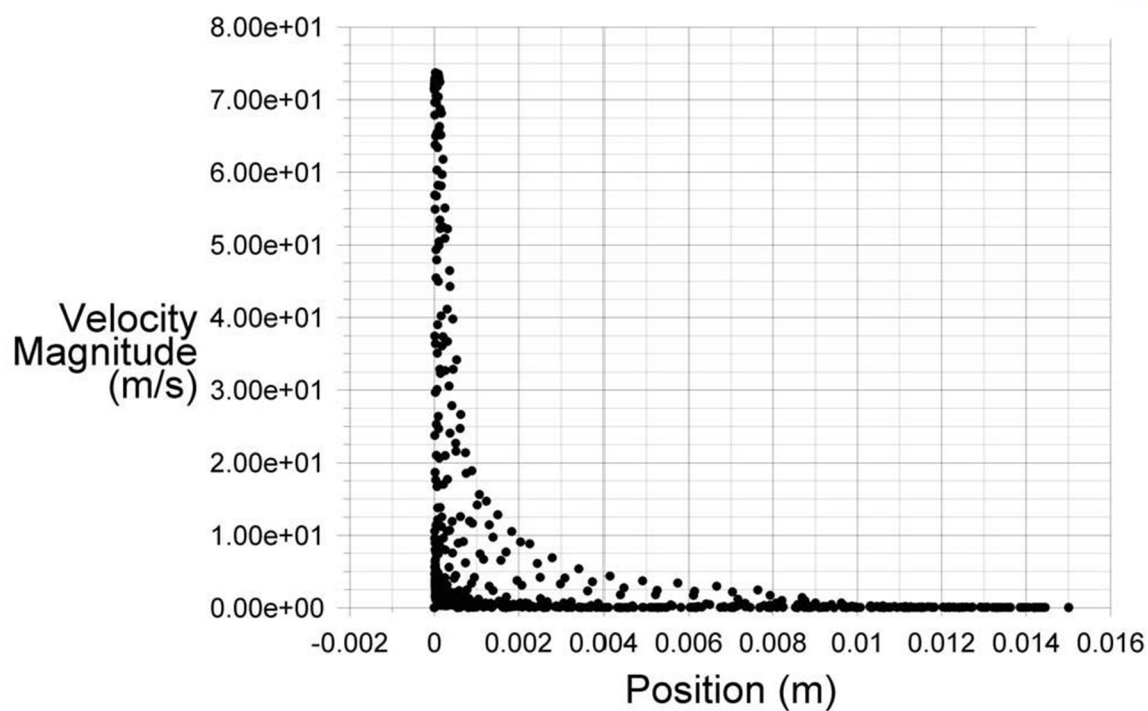


Total Temperature

Aug 09, 2013
ANSYS FLUENT 14.0 (3d, pbns, rke)

• symmetry

ANSYS
14.0



Velocity Magnitude

Aug 09, 2013
ANSYS FLUENT 14.0 (3d, pbns, rke)

0.1 MM DIAMETER (SUPERCRITICAL)

Constants

Sat temperature	194.5 K
Boiling temp	194.5 K
Triple point temp	216.4 K
Surface tension	0.02186 kg/s ²
Density of air	1.225 kg/m ³
Density of vapor CO ₂	1.7878 kg/m ³
Density of liq CO ₂	1032 kg/m ³
Density of solid CO ₂	1562 kg/m ³
Critical weber no.	18
Molar weight	44.01 g/mol
Gas constant	8.314 m ³ Pa/K-mol
Latent heat of vap	571.08 kJ/kg
Latent heat of fusion	196.104 kJ/kg
C _{p,v}	0.8390 kJ/kg-K
C _{p,l}	2.0458 kJ/kg-K
C _{p,s}	1.1580 kJ/kg-K

Aerodynamic break-up (isothermal)

Initial velocity, u	74.3 m/s	
Distance	0.00017 m	
Time	2.288E-06 s	
Droplet velocity	2.653E-06 m/s	Eq. 1
Average diameter	1.333E-05 m	Eq. 2

Thermodynamic break-up

Iteration 1:

CHECK FOR TEMPERATURE

T _{min}	201.60 K	Eq. 5
T _{bulk}	310 K	

NUCLEATION AND BUBBLE GROWTH

Vapor pressure	90 bar	
Flux, Q	592330 g/m ² s	Eq. 4
Radius growth rate	2.414 m/s	Eq. 3
Diameter growth	4.827 m/s	

BLASTING

Starting point	0.00017 m from (0,0)
Initial diameter	1.333E-05 m
Target diameter	2.666E-05 m
Difference	1.333E-05 m
Time taken	2.761E-06 s
Jet velocity	72.5 m/s
Distance travelled	2.002E-04 m
Current distance	0.00037 m from (0,0)

Random number	4.946
Diameter of droplet	6.347E-06 m

Iteration 2:

CHECK FOR TEMPERATURE

T _{min}	209.41 K	Eq. 5
T _{bulk}	277 K	

NUCLEATION AND BUBBLE GROWTH

Vapor pressure	40 bar	
Flux, Q	263258 g/m ² s	Eq. 4
Radius growth rate	1.842 m/s	Eq. 3
Diameter growth	3.684 m/s	

BLASTING

Starting point	0.00037 m from (0,0)
Initial diameter	6.3466E-06 m
Target diameter	1.2693E-05 m
Difference	6.3466E-06 m
Time taken	1.7229E-06 s
Jet velocity	50 m/s
Distance travelled	8.614E-05 m
Current distance	0.00046 m from (0,0)

Random number	4.946
Diameter of droplet	3.0222E-06 m

Iteration 3:

CHECK FOR TEMPERATURE

T _{min}	225.81 K	Eq. 5
T _{bulk}	260 K	

NUCLEATION AND BUBBLE GROWTH

Vapor pressure	25 bar	Eq. 4
Flux, Q	164536 g/m ² s	
Radius growth rate	1.575 m/s	Eq. 3
Diameter growth	3.150 m/s	

BLASTING

Starting point	0.00046 m from (0,0)
Initial diameter	3.0222E-06 m
Target diameter	6.0444E-06 m
Difference	3.0222E-06 m
Time taken	9.5955E-07 s
Jet velocity	45 m/s
Distance travelled	4.318E-05 m
Current distance	0.00050 m from (0,0)

Random number	4.946
Diameter of droplet	1.4391E-06 m

Iteration 4:

CHECK FOR TEMPERATURE

T _{min}	260.25 K	Eq. 5
T _{bulk}	254 K	

NUCLEATION AND BUBBLE GROWTH

Vapor pressure	20 bar	Eq. 4
Flux, Q	131629 g/m ² s	
Radius growth rate	1.575 m/s	Eq. 3
Diameter growth	3.150 m/s	

BLASTING

Starting point	0.00050 m from (0,0)
Initial diameter	1.4391E-06 m
Target diameter	2.8783E-06 m
Difference	1.4391E-06 m
Time taken	4.5693E-07 s
Jet velocity	42 m/s
Distance travelled	1.919E-05 m
Current distance	0.00052 m from (0,0)

Random number	4.946
Diameter of droplet	7.0202E-07 m

Iteration 4:

CHECK FOR TEMPERATURE

T _{min}	329.29 K	Eq. 5
T _{bulk}	252 K	

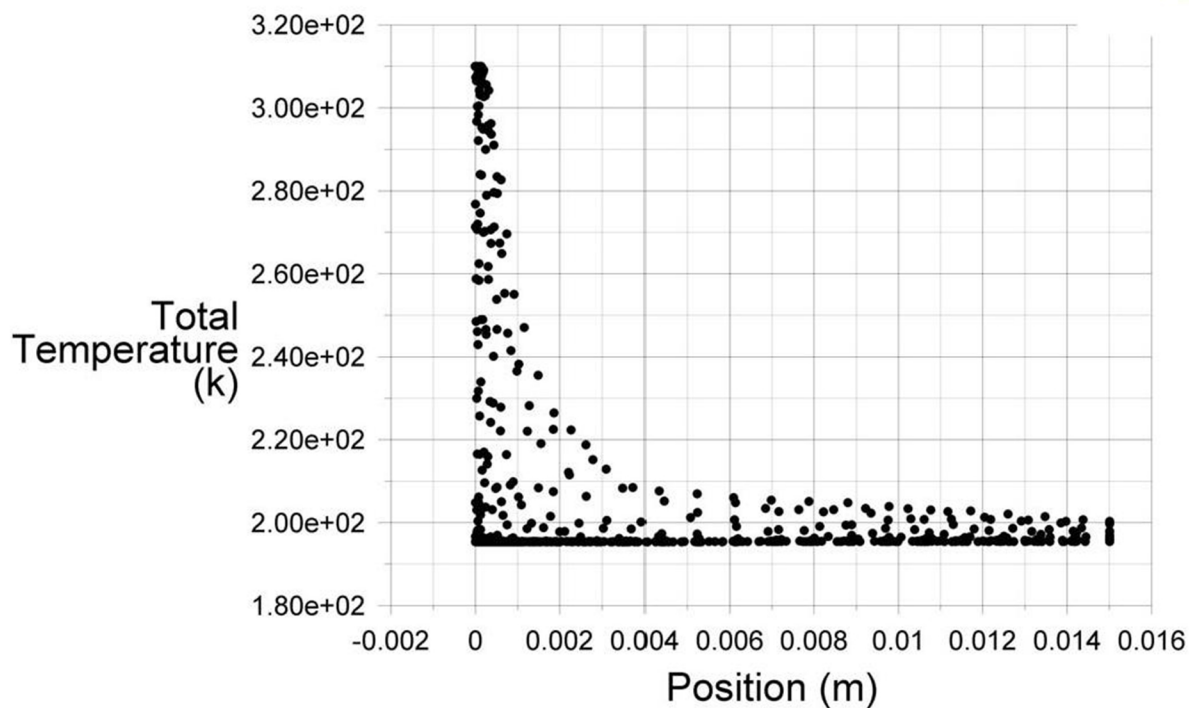
Evaporation and Solidification

Final diameter	6.037E-07 m	Eq. 6
----------------	-------------	-------

0.2 MM DIAMETER (SUPERCRITICAL)

• symmetry

ANSYS
14.0

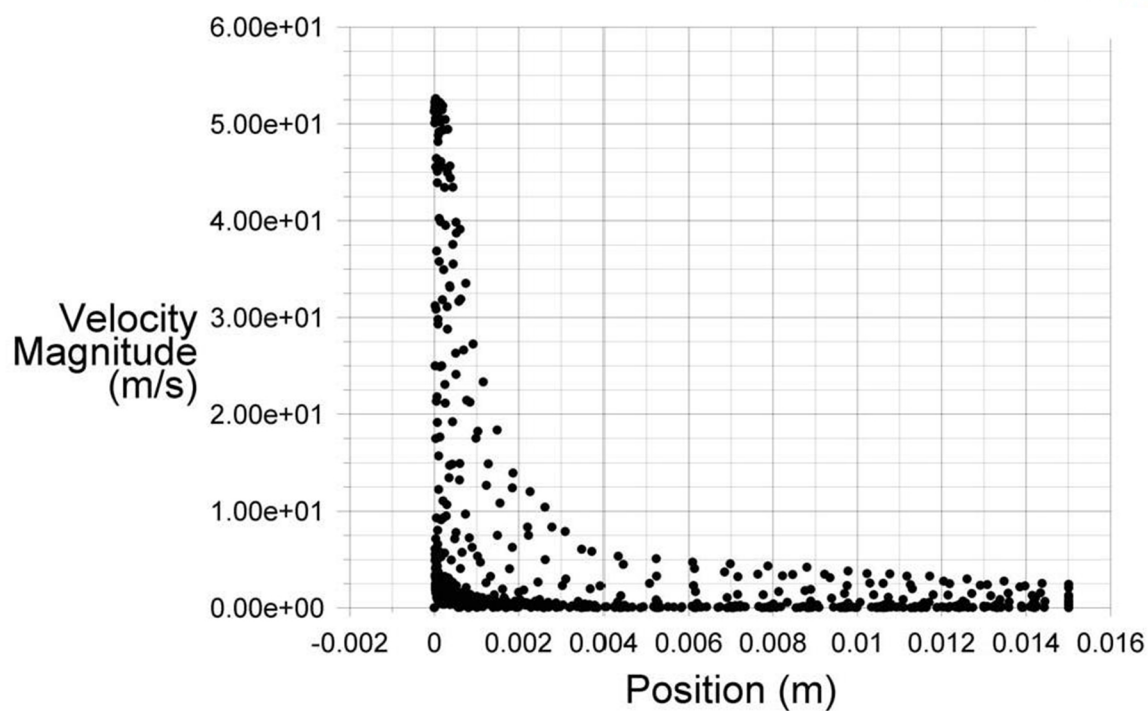


Total Temperature

Aug 08, 2013
ANSYS FLUENT 14.0 (3d, pbns, rke)

• symmetry

ANSYS
14.0



Velocity Magnitude

Aug 08, 2013
ANSYS FLUENT 14.0 (3d, pbns, rke)

0.2 MM DIAMETER

Constants

Sat temperature	194.5 K
Boiling temp	194.5 K
Triple point temp	216.4 K
Surface tension	0.02186 kg/s ²
Density of air	1.225 kg/m ³
Density of vapor CO ₂	1.7878 kg/m ³
Density of liq CO ₂	1032 kg/m ³
Density of solid CO ₂	1562 kg/m ³
Critical weber no.	18
Molar weight	44.01 g/mol
Gas constant	8.314 m ³ Pa/K-mol
Latent heat of vap	571.08 kJ/kg
Latent heat of fusion	196.104 kJ/kg
Cp,v	0.8390 kJ/kg-K
Cp,l	2.0458 kJ/kg-K
Cp,s	1.1580 kJ/kg-K

Aerodynamic break-up (isothermal)

Initial velocity, u	52.5 m/s	
Distance	0.00020 m	
Time	3.810E-06 s	
Droplet velocity	3.122E-06 m/s	Eq. 1
Average diameter	2.669E-05 m	Eq. 2

Thermodynamic break-up

Iteration 1:

CHECK FOR TEMPERATURE

T _{min}	198.04 K	Eq. 5
T _{bulk}	310 K	

NUCLEATION AND BUBBLE GROWTH

Vapor pressure	90 bar	
Flux, Q	592330 g/m ² s	Eq. 4
Radius growth rate	2.414 m/s	Eq. 3
Diameter growth	4.827 m/s	

BLASTING

Starting point	0.00020 m from (0,0)
Initial diameter	2.669E-05 m
Target diameter	5.339E-05 m
Difference	2.669E-05 m
Time taken	5.5301E-06 s
Jet velocity	52 m/s
Distance travelled	2.876E-04 m
Current distance	0.00049 m from (0,0)

Random number	4.946
Diameter of droplet	1.0794E-05 m

Iteration 2:

CHECK FOR TEMPERATURE

T _{min}	203.27 K	Eq. 5
T _{bulk}	288.3 K	

NUCLEATION AND BUBBLE GROWTH

Vapor pressure	50 bar	
Flux, Q	329072 g/m ² s	Eq. 4
Radius growth rate	1.984 m/s	Eq. 3
Diameter growth	3.968 m/s	

BLASTING

Starting point	0.00049 m from (0,0)
Initial diameter	1.0794E-05 m
Target diameter	2.1589E-05 m
Difference	1.0794E-05 m
Time taken	2.7202E-06 s
Jet velocity	42.5 m/s
Distance travelled	1.156E-04 m
Current distance	0.00060 m from (0,0)

Random number	4.946
Diameter of droplet	4.3649E-06 m

Iteration 3:

CHECK FOR TEMPERATURE

T _{min}	216.18 K	Eq. 5
T _{bulk}	278 K	

NUCLEATION AND BUBBLE GROWTH

Vapor pressure	40 bar	Eq. 4
Flux, Q	263258 g/m ² s	
Radius growth rate	1.842 m/s	Eq. 3
Diameter growth	3.684 m/s	

BLASTING

Starting point	0.00060 m from (0,0)
Initial diameter	4.3649E-06 m
Target diameter	8.7297E-06 m
Difference	4.3649E-06 m
Time taken	1.1849E-06 s
Jet velocity	38 m/s
Distance travelled	4.503E-05 m
Current distance	0.00065 m from (0,0)

Random number	4.946
Diameter of droplet	1.765E-06 m

Iteration 4:

CHECK FOR TEMPERATURE

T _{min}	248.11 K	Eq. 5
T _{bulk}	276 K	

NUCLEATION AND BUBBLE GROWTH

Vapor pressure	37 bar	Eq. 4
Flux, Q	243513 g/m ² s	
Radius growth rate	1.795 m/s	Eq. 3
Diameter growth	3.589 m/s	

BLASTING

Starting point	0.00065 m from (0,0)
Initial diameter	1.765E-06 m
Target diameter	3.530E-06 m
Difference	1.765E-06 m
Time taken	4.9175E-07 s
Jet velocity	37 m/s
Distance travelled	1.8195E-05 m
Current distance	0.00067 m from (0,0)

Random number	4.946
Diameter of droplet	7.1371E-07 m

Iteration 5:

CHECK FOR TEMPERATURE

T _{min}	327.08 K	Eq. 5
T _{bulk}	274 K	

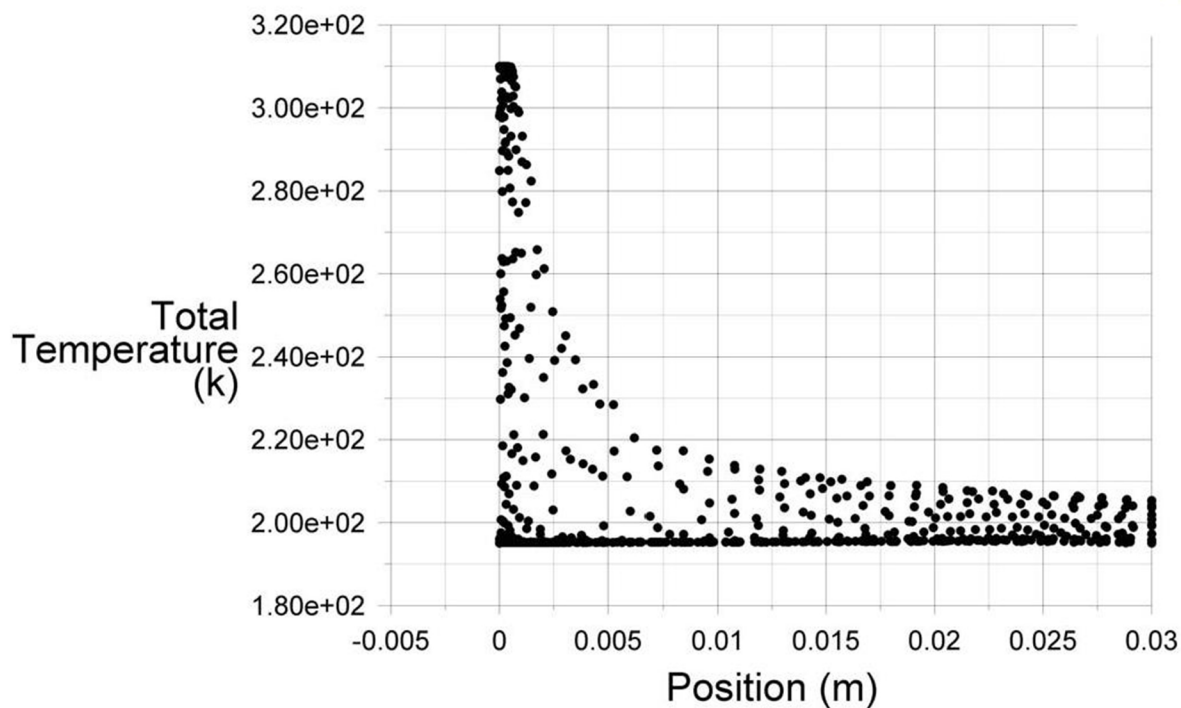
Evaporation and Solidification

Final diameter	6.312E-07 m	Eq. 6
----------------	-------------	-------

0.5 MM DIAMETER (SUPERCRITICAL)

• symmetry

ANSYS
14.0

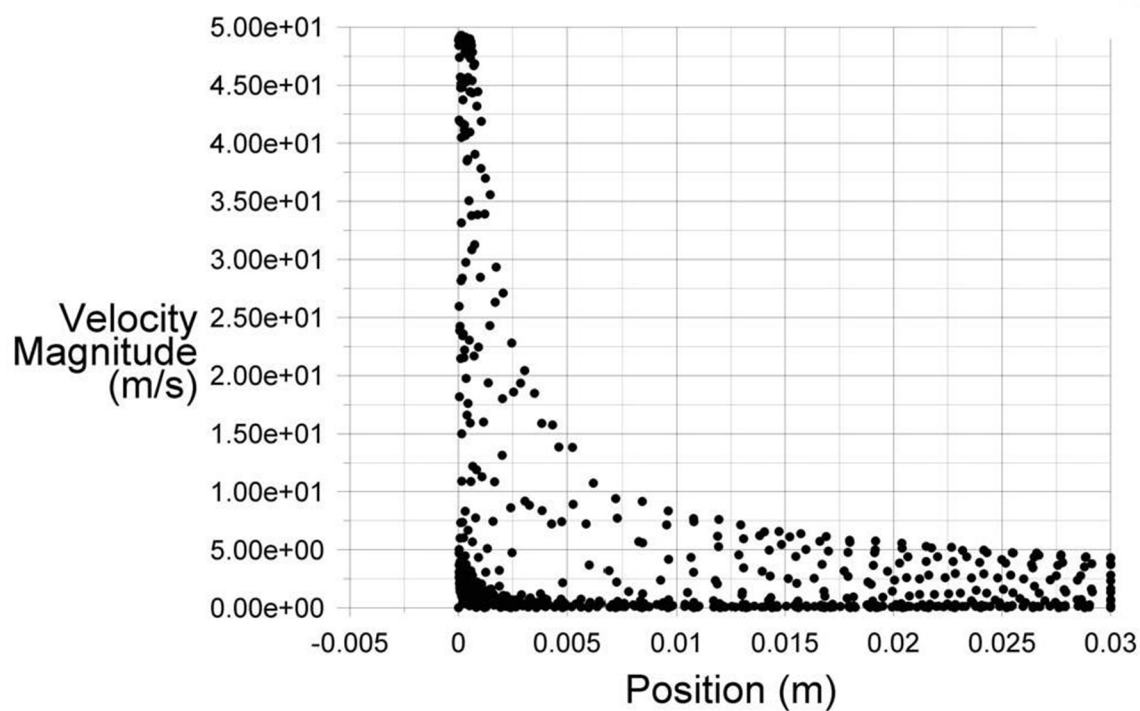


Total Temperature

Aug 08, 2013
ANSYS FLUENT 14.0 (3d, pbns, rke)

• symmetry

ANSYS
14.0



Velocity Magnitude

Aug 08, 2013
ANSYS FLUENT 14.0 (3d, pbns, rke)

0.5 MM DIAMETER

Constants

Sat temperature	194.5 K
Boiling temp	194.5 K
Triple point temp	216.4 K
Surface tension	0.02186 kg/s ²
Density of air	1.225 kg/m ³
Density of vapor CO ₂	1.7878 kg/m ³
Density of liq CO ₂	1032 kg/m ³
Density of solid CO ₂	1562 kg/m ³
Critical weber no.	18
Molar weight	44.01 g/mol
Gas constant	8.314 m ³ Pa/K-mol
Latent heat of vap	571.08 kJ/kg
Latent heat of fusion	196.104 kJ/kg
C _{p,v}	0.8390 kJ/kg-K
C _{p,l}	2.0458 kJ/kg-K
C _{p,s}	1.1580 kJ/kg-K

Aerodynamic break-up (isothermal)

Initial velocity, u	49.5 m/s	
Distance	0.00065 m	
Time	1.313E-05 s	
Droplet velocity	1.015E-05 m/s	Eq. 1
Average diameter	3.003E-05 m	Eq. 2

Thermodynamic break-up

Iteration 1:

CHECK FOR TEMPERATURE

T _{min}	197.65 K	Eq. 5
T _{bulk}	310 K	

NUCLEATION AND BUBBLE GROWTH

Vapor pressure	90 bar	
Flux, Q	592330 g/m ² s	Eq. 4
Radius growth rate	2.414 m/s	Eq. 3
Diameter growth	4.827 m/s	

BLASTING

Starting point	0.00065 m from (0,0)
Initial diameter	3.003E-05 m
Target diameter	6.006E-05 m
Difference	3.003E-05 m
Time taken	6.2207E-06 s
Jet velocity	49 m/s
Distance travelled	3.048E-04 m
Current distance	0.00095 m from (0,0)

Random number	4.946
Diameter of droplet	1.2142E-05 m

Iteration 2:

CHECK FOR TEMPERATURE

T _{min}	202.29 K	Eq. 5
T _{bulk}	298 K	

NUCLEATION AND BUBBLE GROWTH

Vapor pressure	65 bar	
Flux, Q	427794 g/m ² s	Eq. 4
Radius growth rate	2.165 m/s	Eq. 3
Diameter growth	4.331 m/s	

BLASTING

Starting point	0.00095 m from (0,0)
Initial diameter	1.2142E-05 m
Target diameter	2.4285E-05 m
Difference	1.2142E-05 m
Time taken	2.8037E-06 s
Jet velocity	44 m/s
Distance travelled	1.234E-04 m
Current distance	0.00108 m from (0,0)

Random number	4.946
Diameter of droplet	4.91E-06 m

Iteration 3:

CHECK FOR TEMPERATURE

T _{min}	213.77 K	Eq. 5
T _{bulk}	292 K	

NUCLEATION AND BUBBLE GROWTH

Vapor pressure	55 bar	Eq. 4
Flux, Q	361979 g/m ² s	
Radius growth rate	2.048 m/s	Eq. 3
Diameter growth	4.096 m/s	

BLASTING

Starting point	0.00108 m from (0,0)
Initial diameter	4.91E-06 m
Target diameter	9.82E-06 m
Difference	4.91E-06 m
Time taken	1.1986E-06 s
Jet velocity	40 m/s
Distance travelled	4.795E-05 m
Current distance	0.00113 m from (0,0)

Random number	4.946
Diameter of droplet	1.9854E-06 m

Iteration 4:

CHECK FOR TEMPERATURE

T _{min}	242.16 K	Eq. 5
T _{bulk}	290 K	

NUCLEATION AND BUBBLE GROWTH

Vapor pressure	50 bar	Eq. 4
Flux, Q	329072 g/m ² s	
Radius growth rate	1.984 m/s	Eq. 3
Diameter growth	3.968 m/s	

BLASTING

Starting point	0.00113 m from (0,0)
Initial diameter	1.9854E-06 m
Target diameter	3.971E-06 m
Difference	1.9854E-06 m
Time taken	5.0033E-07 s
Jet velocity	38 m/s
Distance travelled	1.9013E-05 m
Current distance	0.00115 m from (0,0)

Random number	4.946
Diameter of droplet	8.0284E-07 m

Iteration 5:

CHECK FOR TEMPERATURE

T _{min}	312.36 K	Eq. 5
T _{bulk}	289 K	

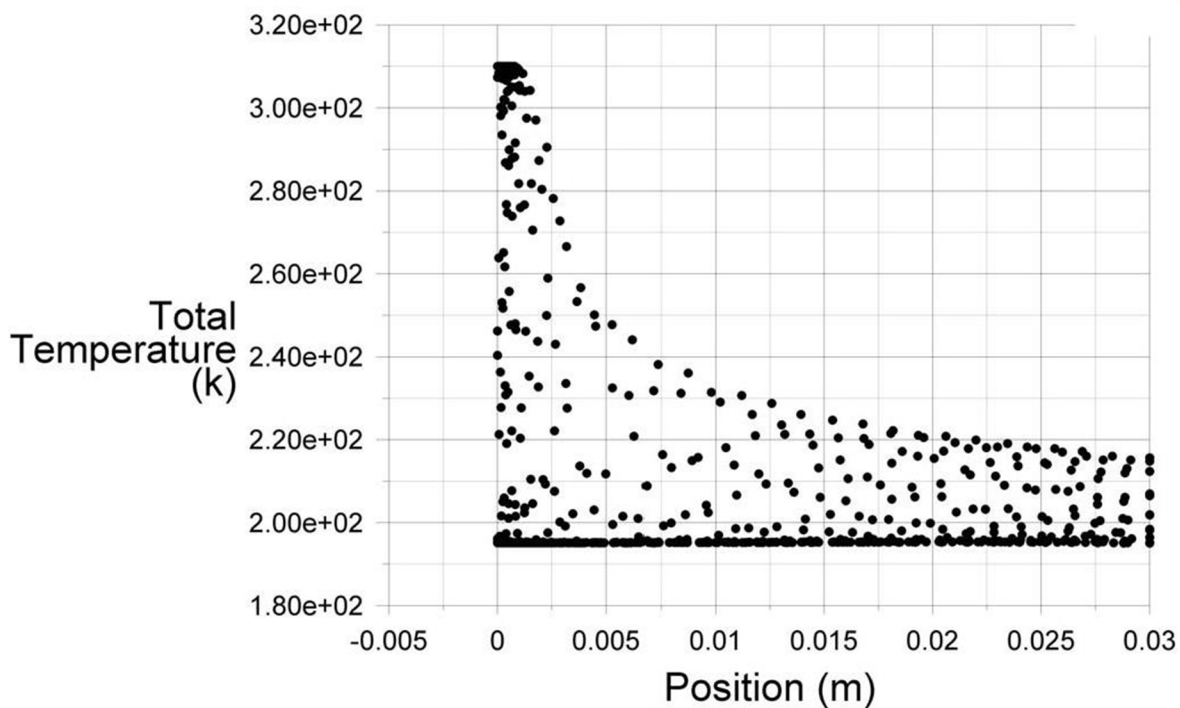
Evaporation and Solidification

Final diameter	7.227E-07 m	Eq. 6
----------------	-------------	-------

1 MM DIAMETER (SUPERCRITICAL)

• symmetry

ANSYS
14.0

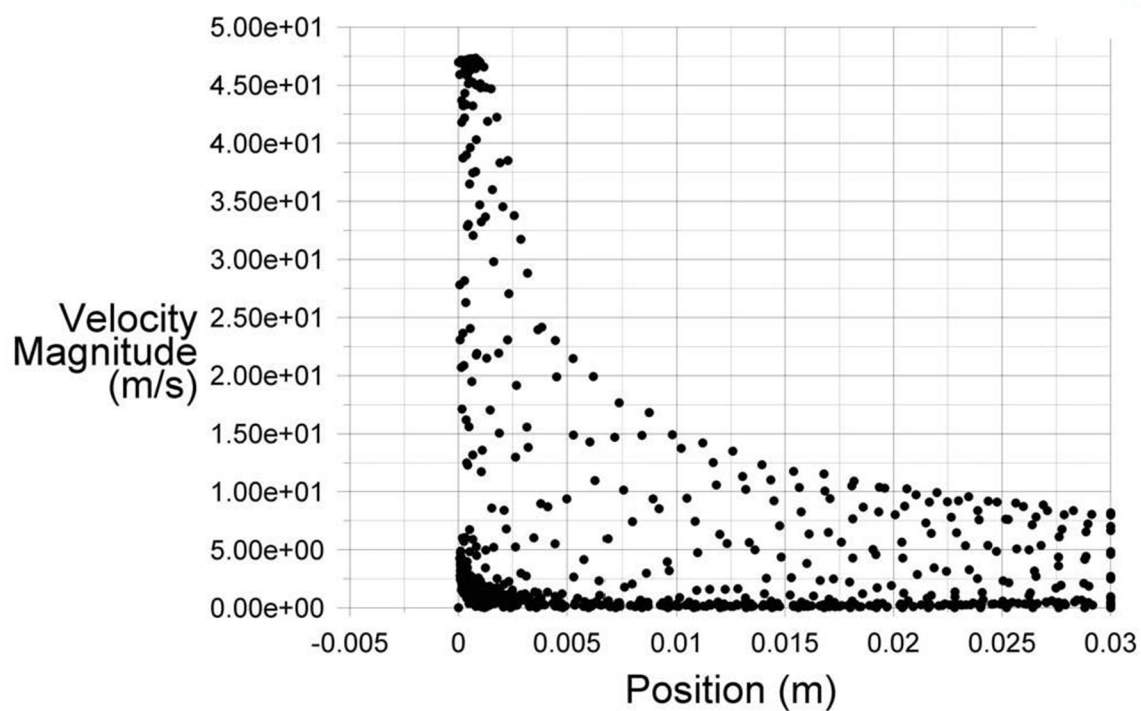


Total Temperature

Aug 08, 2013
ANSYS FLUENT 14.0 (3d, pbns, rke)

• symmetry

ANSYS
14.0



Velocity Magnitude

Aug 08, 2013
ANSYS FLUENT 14.0 (3d, pbns, rke)

1 MM DIAMETER

Constants

Sat temperature	194.5 K
Boiling temp	194.5 K
Triple point temp	216.4 K
Surface tension	0.02186 kg/s ²
Density of air	1.225 kg/m ³
Density of vapor CO ₂	1.7878 kg/m ³
Density of liq CO ₂	1032 kg/m ³
Density of solid CO ₂	1562 kg/m ³
Critical weber no.	18
Molar weight	44.01 g/mol
Gas constant	8.314 m ³ Pa/K-mol
Latent heat of vap	571.08 kJ/kg
Latent heat of fusion	196.104 kJ/kg
C _{p,v}	0.8390 kJ/kg-K
C _{p,l}	2.0458 kJ/kg-K
C _{p,s}	1.1580 kJ/kg-K

Aerodynamic break-up (isothermal)

Initial velocity, u	47.5 m/s	
Distance	0.00097 m	
Time	2.042E-05 s	
Droplet velocity	1.514E-05 m/s	Eq. 1
Average diameter	3.261E-05 m	Eq. 2

Thermodynamic break-up

Iteration 1:

CHECK FOR TEMPERATURE

T _{min}	197.40 K	Eq. 5
T _{bulk}	310 K	

NUCLEATION AND BUBBLE GROWTH

Vapor pressure	90 bar	
Flux, Q	592330 g/m ² s	Eq. 4
Radius growth rate	2.414 m/s	Eq. 3
Diameter growth	4.827 m/s	

BLASTING

Starting point	0.00097 m from (0,0)
Initial diameter	3.261E-05 m
Target diameter	6.522E-05 m
Difference	3.261E-05 m
Time taken	6.7556E-06 s
Jet velocity	48 m/s
Distance travelled	3.243E-04 m
Current distance	0.00129 m from (0,0)

Random number	4.946
Diameter of droplet	1.3186E-05 m

Iteration 2:

CHECK FOR TEMPERATURE

T _{min}	201.68 K	Eq. 5
T _{bulk}	307 K	

NUCLEATION AND BUBBLE GROWTH

Vapor pressure	80 bar	
Flux, Q	526515 g/m ² s	Eq. 4
Radius growth rate	2.321 m/s	Eq. 3
Diameter growth	4.641 m/s	

BLASTING

Starting point	0.00129 m from (0,0)
Initial diameter	1.3186E-05 m
Target diameter	2.6373E-05 m
Difference	1.3186E-05 m
Time taken	2.8411E-06 s
Jet velocity	46 m/s
Distance travelled	1.307E-04 m
Current distance	0.00142 m from (0,0)

Random number	4.946
Diameter of droplet	5.3322E-06 m

Iteration 3:

CHECK FOR TEMPERATURE

T _{min}	212.25 K	Eq. 5
T _{bulk}	305 K	

NUCLEATION AND BUBBLE GROWTH

Vapor pressure	75 bar	Eq. 4
Flux, Q	493608 g/m ² s	
Radius growth rate	2.271 m/s	Eq. 3
Diameter growth	4.542 m/s	

BLASTING

Starting point	0.00142 m from (0,0)
Initial diameter	5.3322E-06 m
Target diameter	1.0664E-05 m
Difference	5.3322E-06 m
Time taken	1.1738E-06 s
Jet velocity	45 m/s
Distance travelled	5.282E-05 m
Current distance	0.00148 m from (0,0)

Random number	4.946
Diameter of droplet	2.0707E-06 m

Iteration 4:

CHECK FOR TEMPERATURE

T _{min}	240.20 K	Eq. 5
T _{bulk}	303 K	

NUCLEATION AND BUBBLE GROWTH

Vapor pressure	72 bar	Eq. 4
Flux, Q	473864 g/m ² s	
Radius growth rate	2.241 m/s	Eq. 3
Diameter growth	4.481 m/s	

BLASTING

Starting point	0.00148 m from (0,0)
Initial diameter	2.0707E-06 m
Target diameter	4.141E-06 m
Difference	2.0707E-06 m
Time taken	4.6211E-07 s
Jet velocity	44 m/s
Distance travelled	2.0333E-05 m
Current distance	0.00150 m from (0,0)

Random number	4.946
Diameter of droplet	8.3734E-07 m

Iteration 5:

CHECK FOR TEMPERATURE

T _{min}	307.51 K	Eq. 5
T _{bulk}	300 K	

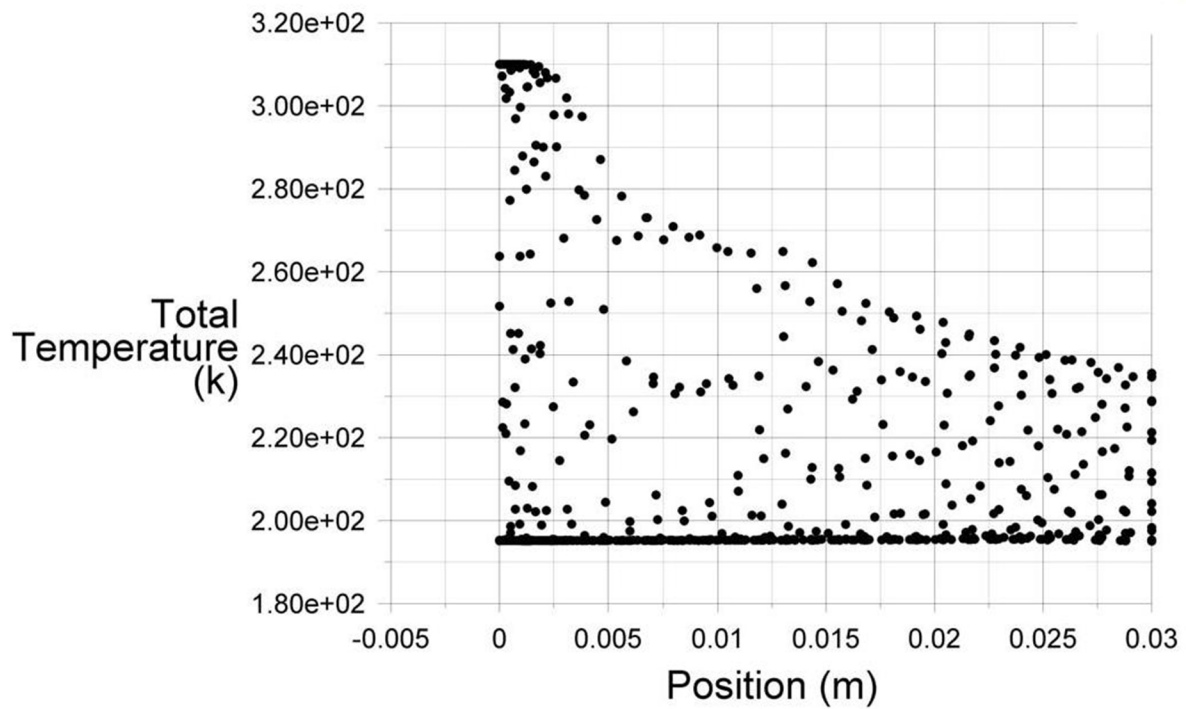
Evaporation and Solidification

Final diameter	7.632E-07 m	Eq. 6
----------------	-------------	-------

2 MM DIAMETER (SUPERCRITICAL)

• symmetry

ANSYS
14.0

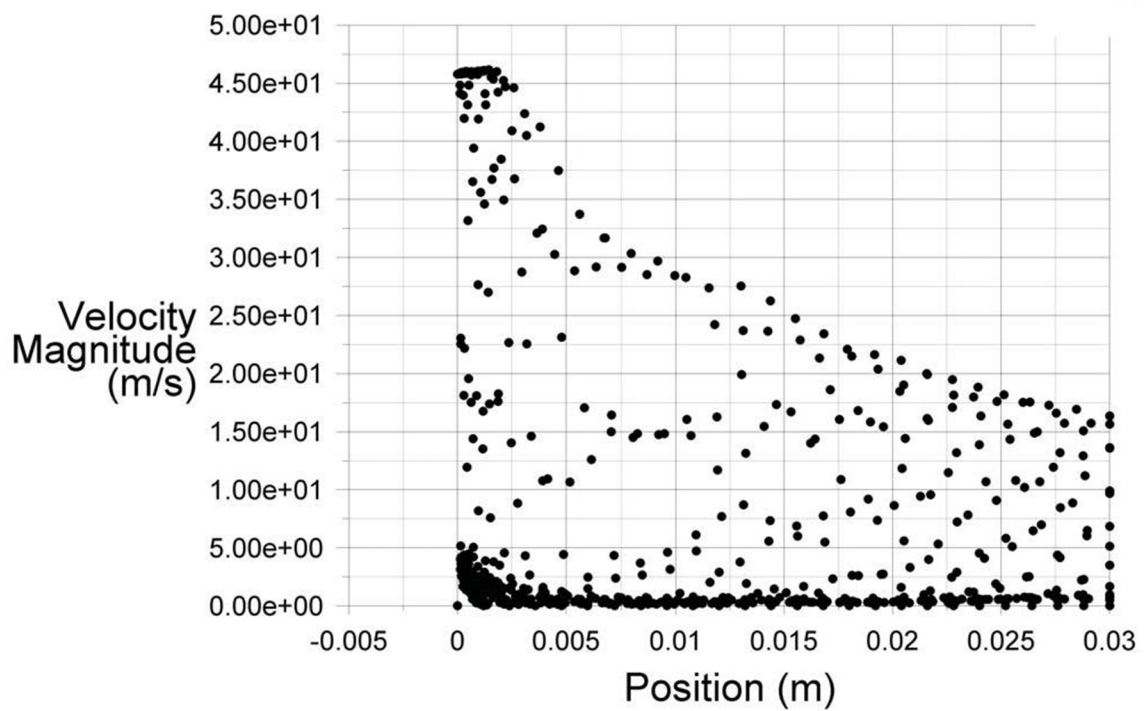


Total Temperature

Jul 29, 2013
ANSYS FLUENT 14.0 (3d, pbns, rke)

• symmetry

ANSYS
14.0



Velocity Magnitude

Aug 08, 2013
ANSYS FLUENT 14.0 (3d, pbns, rke)

2 MM DIAMETER

Constants

Sat temperature	194.5 K
Boiling temp	194.5 K
Triple point temp	216.4 K
Surface tension	0.02186 kg/s ²
Density of air	1.225 kg/m ³
Density of vapor CO ₂	1.7878 kg/m ³
Density of liq CO ₂	1032 kg/m ³
Density of solid CO ₂	1562 kg/m ³
Critical weber no.	18
Molar weight	44.01 g/mol
Gas constant	8.314 m ³ Pa/K-mol
Latent heat of vap	571.08 kJ/kg
Latent heat of fusion	196.104 kJ/kg
Cp,v	0.8390 kJ/kg-K
Cp,l	2.0458 kJ/kg-K
Cp,s	1.1580 kJ/kg-K

Aerodynamic break-up (isothermal)

Initial velocity, u	46.2 m/s	
Distance	0.00161 m	
Time	3.485E-05 s	
Droplet velocity	2.513E-05 m/s	Eq. 1
Average diameter	3.447E-05 m	Eq. 2

Thermodynamic break-up

Iteration 1:

CHECK FOR TEMPERATURE

T _{min}	197.25 K	Eq. 5
T _{bulk}	310 K	

NUCLEATION AND BUBBLE GROWTH

Vapor pressure	90 bar	
Flux, Q	592330 g/m ² s	Eq. 4
Radius growth rate	2.414 m/s	Eq. 3
Diameter growth	4.827 m/s	

BLASTING

Starting point	0.00161 m from (0,0)
Initial diameter	3.447E-05 m
Target diameter	6.894E-05 m
Difference	3.447E-05 m
Time taken	7.1411E-06 s
Jet velocity	46.5 m/s
Distance travelled	3.321E-04 m
Current distance	0.00194 m from (0,0)

Random number	4.946
Diameter of droplet	1.3939E-05 m

Iteration 2:

CHECK FOR TEMPERATURE

T _{min}	201.29 K	Eq. 5
T _{bulk}	308 K	

NUCLEATION AND BUBBLE GROWTH

Vapor pressure	85 bar	
Flux, Q	559422 g/m ² s	Eq. 4
Radius growth rate	2.368 m/s	Eq. 3
Diameter growth	4.736 m/s	

BLASTING

Starting point	0.00194 m from (0,0)
Initial diameter	1.3939E-05 m
Target diameter	2.7878E-05 m
Difference	1.3939E-05 m
Time taken	2.9432E-06 s
Jet velocity	46 m/s
Distance travelled	1.354E-04 m
Current distance	0.00208 m from (0,0)

Random number	4.946
Diameter of droplet	5.6365E-06 m

Iteration 3:

CHECK FOR TEMPERATURE

T _{min}	211.29 K	Eq. 5
T _{bulk}	307 K	

NUCLEATION AND BUBBLE GROWTH

Vapor pressure	80 bar	Eq. 4
Flux, Q	526515 g/m ² s	
Radius growth rate	2.321 m/s	Eq. 3
Diameter growth	4.641 m/s	

BLASTING

Starting point	0.00208 m from (0,0)
Initial diameter	5.6365E-06 m
Target diameter	1.1273E-05 m
Difference	5.6365E-06 m
Time taken	1.2144E-06 s
Jet velocity	45 m/s
Distance travelled	5.465E-05 m
Current distance	0.00213 m from (0,0)

Random number	4.946
Diameter of droplet	2.1679E-06 m

Iteration 4:

CHECK FOR TEMPERATURE

T _{min}	238.15 K	Eq. 5
T _{bulk}	305 K	

NUCLEATION AND BUBBLE GROWTH

Vapor pressure	75 bar	Eq. 4
Flux, Q	493608 g/m ² s	
Radius growth rate	2.271 m/s	Eq. 3
Diameter growth	4.542 m/s	

BLASTING

Starting point	0.00213 m from (0,0)
Initial diameter	2.1679E-06 m
Target diameter	4.336E-06 m
Difference	2.1679E-06 m
Time taken	4.7724E-07 s
Jet velocity	44 m/s
Distance travelled	2.0999E-05 m
Current distance	0.00215 m from (0,0)

Random number	4.946
Diameter of droplet	8.5014E-07 m

Iteration 5:

CHECK FOR TEMPERATURE

T _{min}	305.80 K	Eq. 5
T _{bulk}	303 K	

Evaporation and Solidification

Final diameter	7.775E-07 m	Eq. 6
----------------	-------------	-------